# Chapter 2
# On the Chirality of Doped Liquid Crystals

*In this introductory chapter a literature overview of various aspects of liquid crystal science and technology is given, with a focus on chirality. The first part deals with the wide variety of liquid crystal forms and appearances, and the associated experimental techniques relevant to the research described in this thesis. In the second part of this chapter an overview of the research on chiral, doped liquid crystals is given. Based on a distinction between shape-persistent and bistable dopants, several dopant classes and effects will be discussed.*

## 2.1 Introduction to Liquid Crystal Phases

### 2.1.1 Background

Liquid crystals (LCs) form a unique state of matter. Between the solid (crystalline) and liquid (isotropic) phases some compounds display a distinctly different, intermediate state, also referred to as the *fourth state of matter*, or the *mesophase*. As such, these materials display properties common to both solids and liquids. Due to anisotropic weak intermolecular interactions, the molecules[1], or *mesogens*, in such a liquid crystalline assembly possess some kind of either positional or orientational order, but with a much lower degree of organization than in a crystalline solid. Therefore, the LC phase still shows a liquid-like flowing behavior, although as a result of the higher degree of organization compared to ordinary liquids these materials are much more viscous, and often turbid. Because of this combination of dynamic behavior and high degree of organization, liquid crystals tend to be sensitive to various stimuli, such as temperature, electric and magnetic fields and non-mesogenic molecules dissolved in the liquid crystalline matrix. Combined with their self-assembling behavior, this makes them extremely interesting for both chemistry and physics. Due to their unique properties these materials have found widespread applications in liquid crystal displays (LCDs).

The mesophase was first discovered in 1888 by the Austrian botanist Reinitzer, who was intrigued by the observation that cholesteryl benzoate has two melting points.[2] Together with Lehmann, a German physicist, this phenomenon was further investigated.[3] Much later, it was found that liquid crystals are ubiquitous in Nature as phospholipid cell membranes as well as myelin, a lipid material protecting the nerves, are liquid crystalline. The same holds for some concentrated DNA and protein solutions, like for instance the secretion of a spider that is used to generate silk. Although a rich variety of molecules are known that are prone to form liquid crystalline phases, showing large differences in the degree and kind of orientation, they all have a strongly anisotropic shape in common. Especially elongated rod-like (calamitic) and disc-like (discotic) molecules are known to possess a liquid crystalline state. This strong shape anisotropy is reflected in a strong anisotropy in the organization of the macroscopic liquid crystalline phase and its physical properties.

Liquid crystalline systems can be classified in many ways.[4] Apart from the distinction between calamitic and discotic, one can discriminate between amphiphilic or nonamphiphilic, metal containing or non-metal containing and low molecular weight or polymeric liquid crystals. Moreover, most LC materials

described above show thermotropic behaviour, meaning that they are solvent-free systems, that are liquid crystalline in a limited temperature range. Below this range a thermotropic liquid crystalline substance will form a crystalline phase and above this temperature an isotropic liquid phase exists (Figure 2.1). However, there are also solvent-solute type systems, where the aggregation of the solutes results in liquid crystallinity (lyotropic behavior). The work presented in his thesis will focus on calamitic, thermotropic liquid crystals that are of low molecular weight, non-metal containing and non-amphiphilic. These liquid crystals can be divided into several types of sub-phases that differ in the degree of orientational ordering. Three important sub-phases are smectic (Sm), nematic (N) and cholesteric (N*) (or chiral nematic) (Figure 2.2).

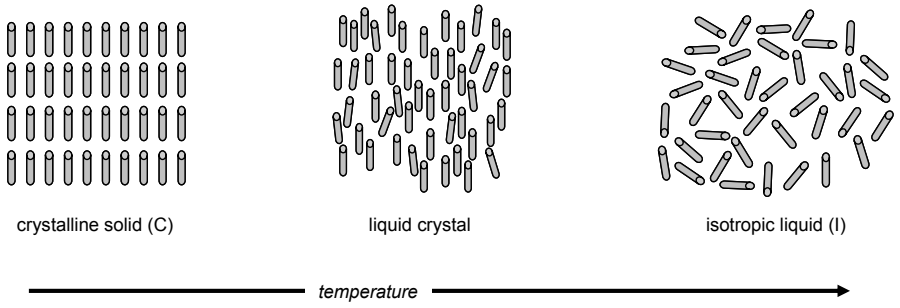


**Figure 2.1** Thermotropic liquid crystal phase transition behavior.

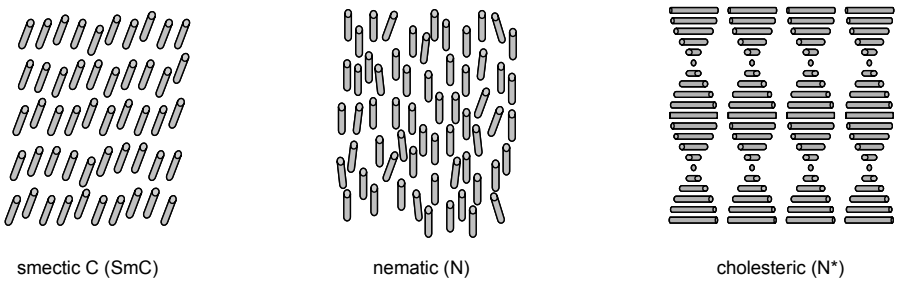


**Figure 2.2** Molecular arrangement of mesogens in common LC subphases.

### 2.1.2 Molecular Order

In the crystalline (solid) state, molecules usually have near-perfect orientational order. In the mesophase this degree of order is partially but not completely lost, as the molecules show highly dynamic behavior and only on average point in the same direction. In fact, the molecules spend little more time pointing along a

common orientation axis than they do in any other direction but they do so sufficiently long enough for there to be orientational order. This preferred direction is called the director (Figure 2.3). The degree of order is described by the order parameter (*S*), which is a measure for the average angle $\theta$ between the director and the long axes of the mesogens (eq. 2.1). For an isotropic sample, $S = 0$, whereas for a perfectly aligned crystal $S = 1$. For a typical liquid crystal, $S$ is between 0.3 to 0.8, and this value generally decreases due to higher mobility and disorder as the temperature is raised.

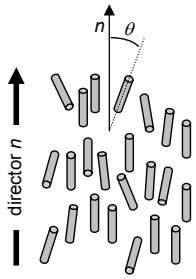


**Figure 2.3** Model structure of the nematic phase and definition of the nematic director *n*. The angle $\theta$ denotes the deviation of the long axis of an individual mesogen from the director.

$$S = \frac{3\cos^2\theta - 1}{2} \qquad \textbf{eq. 2.1}$$

### 2.1.3 Smectic Liquid Crystals

Although of less significance for this thesis, the smectic LC phase is of enormous importance for modern liquid crystal research.[4] Originally discovered with amphiphilic molecules, the phase was named after the Greek σμεκτοσ (smektos meaning soap-like). Nowadays, the name is used for LC phases were, apart from possessing orientational order, the molecules are organized in layers. These layers can slide relative to each other, resulting in highly viscous liquid-like behavior. Many different smectic phases are known, each one differing in orientation and position of the mesogenic molecules.[5] They are distinguished by a letter and denoted as SmA, SmB, SmC, etc. A chiral version of the SmC phase also exists, designated SmC*. In the SmC phase, the molecules in the layered structure are tilted and in the SmC* phase the average orientation of these tilted molecules, exhibits a helical propagation going from layer to layer, resulting in a structure that is not superimposable on its mirror image. As a result of

ferroelectric properties associated with this phase it is considered highly promising for future applications in materials science and display technology.

### 2.1.4 Nematic Liquid Crystals

The simplest liquid crystalline phase possible is the nematic phase (N), as it has only a slight orientational order of the individual mesogens. The molecules can translate freely and can rotate around their long axis, leading to a much lower viscosity than observed for smectic phases. The nematic phase is named after the Greek word νεμα (nema meaning thread) as it often appears to have miniscule threads when observed through a microscope.

### 2.1.5 Cholesteric Liquid Crystals

The cholesteric (or chiral nematic, N*) liquid crystalline phase is essentially a nematic phase with an additional helical change in orientation of the director.

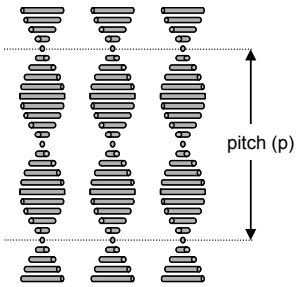


**Figure 2.4** Schematic representation of chiral nematic or cholesteric phase and definition of the cholesteric pitch.

Whereas the director in an ordinary nematic liquid crystal has a constant direction, in a cholesteric phase it changes direction in a helical fashion throughout the sample, perpendicular to the helix axis. The orientation of the director describes a helical propagation along the cholesteric helix axis that is non-superimposable on its mirror image, making it chiral. The resulting supramolecular chirality is indicated by the sign and magnitude of the cholesteric pitch (*p*), which is the distance in the material across which the director rotates a full 360° (Figure 2.4). The name of the cholesteric phase originates from the cholesterol derivatives for which this phenomenon was first observed[2,3], but in principle any chiral nematic phase is referred to as cholesteric.

## 2.2 Chirality in Liquid Crystals

The chirality of the cholesteric liquid crystalline phase is a unique property that has found widespread use in stereochemistry, optics and materials science.[4] Three types of cholesteric systems can be distinguished. The first type consists of collections of mesogenic molecules that have a stereogenic centre in their molecular structure (e.g. cholesteryl benzoate) and can form liquid crystalline phases with a helical ordering. In the second type, chiral guest molecules are dissolved in an achiral nematic host, as a result of which all the achiral mesogens take up the chiral cholesteric orientation. The third type is the so called twisted nematic, which can be found in liquid crystal displays. It does not have to contain chiral molecules as the liquid crystal molecules adopt a 90° helical twist by sandwiching them between two perpendicular alignment layers (Figure 2.5).

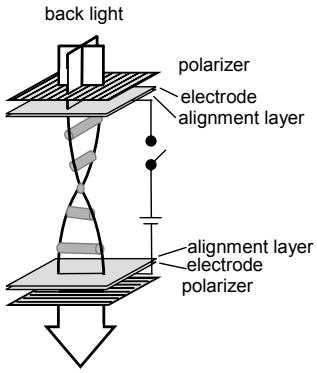


**Figure 2.5** Schematic representation of a twisted nematic liquid crystal cell with a left-handed cholesteric phase.

### 2.2.1 Doped Liquid Crystals

Doped liquid crystals, obtained by dissolving a chiral guest (the dopant) in a nematic host, have many interesting properties.[6] The nature of the induced cholesteric phase is highly dependent on the properties of the chiral dopant; this is reflected both in the sign as well as the magnitude of the cholesteric pitch. The efficiency of the dopant to induce a helical organization in a liquid crystalline matrix is expressed in a parameter known as the helical twisting power ($\beta$). This parameter, intrinsic to every chiral compound and different for every host-guest combination, reflects the amount of dopant needed to reach a cholesteric phase with a certain pitch. The pitch then is inversely proportional to the

concentration (*c*), the helical twisting power and the enantiomeric excess (*ee*) of the dopant (eq. 2.2).

$$p = \frac{1}{c \cdot \beta \cdot ee} \qquad \textbf{eq. 2.2}$$

Compared to cholesteric LCs made up of chiral mesogens, doped liquid crystals offer some major advantages. Most important, the pitch of the material is easily tuned by changing the host-guest ratio or the nature of the guest. Chiral guests can be synthesized separately, after which the nematic host and the chiral guest can self assemble to form a cholesteric liquid crystalline phase. Moreover, the molecular chirality of the guest is amplified in the supramolecular helix structure.

### 2.2.2 Amplification of Chirality in Liquid Crystals

Cholesteric liquid crystals are characterized by large supramolecular chiral organization and as a result these materials display very large optical and circular dichroism (CD) activities.[7] These optical and CD activities can be orders of magnitude higher than that of the dopant, thereby amplifying the dopant's chirality. A typical example is menthol, which has a 30,000 times larger specific molar optical rotation in LC host MBBA ($[\phi]_{578} \sim 2{,}400{,}000°$, see Section 2.3.3 for the structure of MBBA) than in ethanol ($[\phi]_D = 78°$).[8] In addition these chiral LCs show macroscopic chiral properties that can be used as a measure of their chiral organization, and therefore indirectly as a measure of the chirality of the dopant. These macroscopic properties are explained in Sections 2.2.3, 2.2.4 and 2.3.2.

### 2.2.3 Determination of the Cholesteric Pitch

The common method for determination of the cholesteric pitch, and thereby also indirectly the helical twisting power, is the Grandjean-Cano technique.[4a,9] A cholesteric LC sample is aligned between a flat surface and a plane convex lens of known diameter R, and a series of concentric disclination lines will appear under these conditions (Figure 2.6). The difference in radius (r) of two consecutive lines is a measure for the pitch of the cholesteric helix, via equation 2.3. Using equation 2.2 the helical twisting power of the dopant can then be determined.

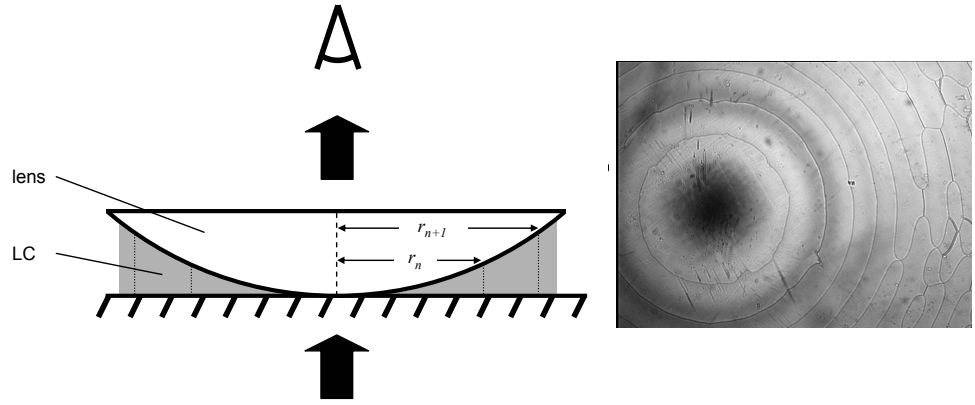


**Figure 2.6** Setup for determination of the cholesteric pitch using the Grandjean-Cano lens method; Grandjean-Cano disclinations observed through an optical microscope when applying this method.

$$p = \frac{r_{n+1}^2 - r_n^2}{R_{lens}}, \text{ n} = 1, 2, 3,\ldots \qquad \textbf{eq. 2.3}$$

Other ways of determining the pitch are for instance the method described in Section 2.2.4, using the selective reflection of light by aligned cholesteric phases, or distance measurements in cholesteric fingerprint textures as described in Section 2.3.2. However, the former method has the major disadvantage that it is necessary to generate a cholesteric phase with a sub-micrometer pitch, which is not always feasible. In the case of the fingerprint method it was shown that the measured pitch is highly dependent on the alignment surface employed, making comparison between different measurements impossible.[10]

### 2.2.4 Optical Properties of Cholesteric Liquid Crystals

Cholesteric liquid crystals can be colored when the length of their helical pitch is of the same order of magnitude as the wavelength of visible light. This color is not the result of absorption, as it is for conventional dyes and pigments, but of selective reflection. The cholesteric phase, when illuminated with white light, reflects light of a certain wavelength depending on the helical pitch of the material (Figure 2.7). The non-reflected light is transmitted through the LC film.[11] Moreover, the reflected and transmitted light will become circularly polarized, with their signs depending on the sign of the cholesteric helix. The reflected light of a left-handed helix will be left-handed (*l*-CPL), the transmitted light is right-handed circularly polarized (*r*-CPL).

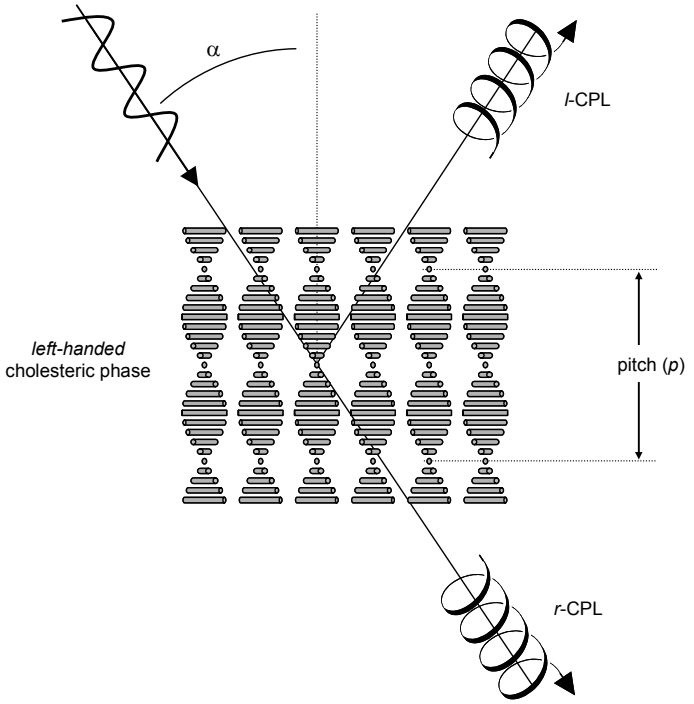


**Figure 2.7** A cholesteric phase and its optical properties.

The selective reflection is of a Bragg-type, resulting from the repetitive helical order in the cholesteric phase.[12] When perpendicular to the surface, the wavelength of reflection ($\lambda_{\perp}$) is dependent on the pitch ($p$) and the mean refractive index ($n$) of the material (eq. 2.4a).

$$\lambda_{\perp} = n \cdot p \qquad \textbf{eq. 2.4a}$$

As the color is also strongly dependent on the viewing angle, the angle dependency of the wavelength of reflection is described in equation 2.4b, with $\alpha$ being the angle of incident light relative to the normal. Equation 2.4b reduces to equation 2.4a when $\alpha = 0°$.[6d]

$$\lambda(\alpha) = n \cdot p \cdot \cos\left( \sin^{-1} \frac{\sin \alpha}{n} \right) \qquad \textbf{eq. 2.4b}$$

As the pitch, which causes the color of the cholesteric phase, is dependent on the properties of the chiral dopant, the color of a doped LC can be influenced by changing the concentration, enantiomeric excess or helical twisting power of the

dopant. This offers the possibility of generating many different colors with a single dopant, something which is not possible with a dye. This can also be achieved using a dopant in which the helical twisting powers can be modulated, allowing selective color change of a single film. Applications of this principle will be described in Chapter 6. Furthermore, the color of the film can serve as a measure for the enantiomeric excess of the dopant, as will be described in Chapter 3.

Besides the selective light reflection, a property exclusive for chiral liquid crystalline phases, all LC phases display birefringence.[4] As a result of the anisotropic supramolecular structure, the index of refraction depends on the direction of light propagation. This leads to various optical effects when observing an LC phase through a polarization microscope.[4a]

## 2.3 Liquid Crystal Phases, Structures and Textures

The properties of a liquid crystalline phase are a result of the aggregation behavior of the mesogens, as well as the orientation of the director with respect to the surface of the substrate. As such, it is important to control both the modes of aggregation and orientation, using liquid crystalline films aligned on surfaces or in cells.

### 2.3.1 Alignment

The orientation of the director with respect to the surface is highly dependent on the structure of this surface. Furthermore, many properties of liquid crystalline films can only be applied when the bulk material is aligned in a specific orientation. For this purpose, many ways of aligning liquid crystalline films on surfaces have been developed. Traditionally, the fabrication of such surfaces involves the mechanical rubbing of polymers, which have been spin-coated onto substrates like glass or indium-tin oxide. This rubbing creates microscopic grooves on the surface, which form an alignment layer that causes the LCs to align in the direction of rubbing. Polyimides are commonly used for this, as they are chemically quite inert, transparent in the visible spectrum, show excellent adhesion to substrates and are thermally stable. Recently various new methods of alignment have been developed, including micro rubbing,[13] self-assembled monolayers,[14] supramolecular nanogroove amplification,[15] ion-beam lithography[16] and several methods using linearly polarized light, with the purpose of generation more uniform alignment, using less invasive techniques in cleaner surroundings.[17] However, all the work described in this thesis is based on the

traditional mechanical rubbing technique, as it is easy to perform and usually gave satisfactory results.

### 2.3.2 Structure of Liquid Crystals on Surfaces

Two modes of nematic LC alignment are normally found: *planar*, with the director parallel to the surface, and *homeotropic*, where the director is perpendicular (Figure 2.8). A rubbed polyimide-coated substrate will normally force a nematic LC film in a planar orientation, whereas homeotropic alignment can be achieved using for instance surfactant or silane coated surfaces. In cholesterics the orientation is based on the direction of the helix axis, as the orientation of the director is not constant. Three arrangements can be distinguished: *planar*, with the cholesteric helix perpendicular to the surface; *polygonal (fingerprint)*, with the helix axis parallel to the surface; and *focal conic*, where there is a random distribution of the helix axis (Figure 2.9).

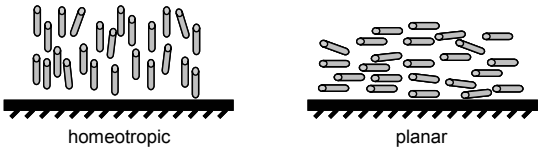


**Figure 2.8** Mesogenic orientation of nematic phase.

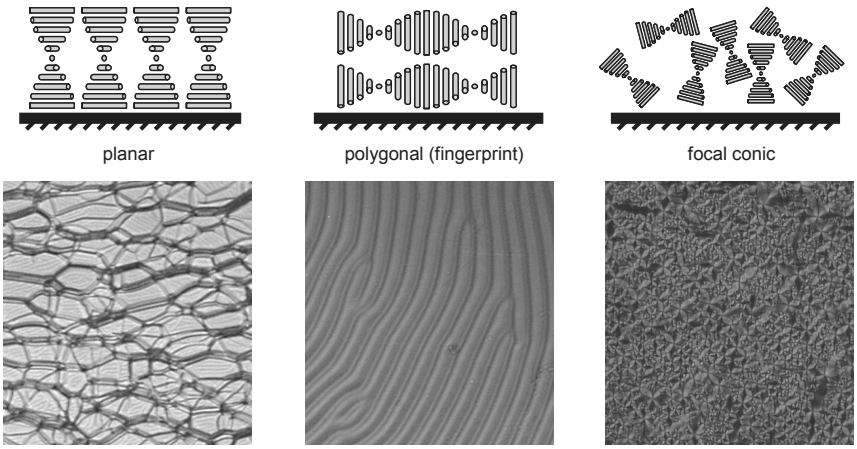


**Figure 2.9** Mesogenic orientation of cholesteric phase and corresponding textures.

The fingerprint texture provides a side-on view of the cholesteric helix. As a result of the rotation of the director, the refractive index varies in an oscillatory

manner. Under an optical microscope with crossed polarizers, this appears as a striped texture, where the distance between two bands is equal to half the pitch.[18] In order to selectively reflect light, as described in Section 2.2.4, a cholesteric film has to have a planar or focal conic orientation.[6d]

### 2.3.3 Liquid Crystal Hosts

An enormous variety of mesogenic molecules is known and several are commercially available. They are often applied as mixtures of a number of similar mesogens, in order to broaden the liquid crystalline temperature range (eutectic) and for fine-tuning of specific physical properties. As the properties of a liquid crystalline phase depend highly on the mesogen employed, an overview of the structures of some widely applied mesogens is given in Table 2.1.

**Table 2.1** Chemical structures and phase transitions of common LC hosts.

| Name | Structure[a] | Phase transitions[b] |
|---|---|---|
| MBBA | 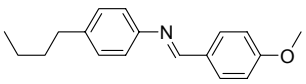 | $C\ \overset{20}{}\ N\ \overset{47}{}\ I$ |
| ZLI-1167 | 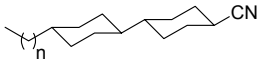 | n.a. |
| | eutectic mixture, n = 2, 4, 6. | |
| ZLI-389 | alkoxyphenylpentylbenzoates, mixture | $C\ \overset{-65}{}\ N\ \overset{35}{}\ I$ |
| | exact composition n.a. | |
| K15 | 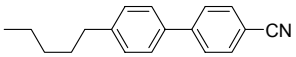 | $C\ \overset{22.5}{}\ N\ \overset{35}{}\ I$ |
| pCH7 | 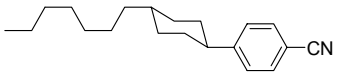 | $C\ \overset{30}{}\ N\ \overset{59}{}\ I$ |
| E7 | 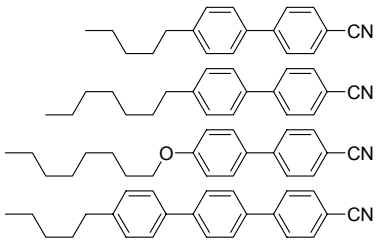 | $C\ \overset{-10}{}\ N\ \overset{60}{}\ I$ |

[a] n.a. = not available; [b] *C* = crystalline, *N* = nematic, *I* = isotropic; numbers indicate phase transition temperatures in °C.

## 2.4 Dopants

The properties of a cholesteric LC phase are a direct result of its helical ordering. In the case of doped liquid crystals, the helical order is caused by the interaction of a chiral guest molecule (the dopant) with an achiral nematic host, which can be expressed in the dopants helical twisting power (eq. 2.2). As this principle is the basis for the work described in this thesis, a concise discussion of previous research on chiral doped liquid crystals is required.

Over the last 25 years, doped liquid crystal research has split up into two major fields. The first focuses on the development of shape persistent dopants, mainly aiming at reaching high helical twisting powers and investigation of the interactions between chiral dopants and LC host molecules.[19] In the second field the focus lies on the development of switchable dopants, which can change shape in reaction to an external stimulus, usually light or heat.[20] In this area the focus lies more on future application, for instance in liquid crystal displays.

### 2.4.1 Shape Persistent Dopants

Typical commercially available chiral compounds have rather low helical twisting powers, mostly due to shape, size, polarization, or conformational incompatibility with the LC host. Therefore, specially designed molecules have been tested for their interaction with liquid crystalline hosts. Based on their structure, these dopants can roughly be divided in four classes.

#### *2.4.1.1 Mesogenic functionalization*

The most straightforward way of designing a suitable chiral dopant is to functionalize a chiral molecule with a liquid crystal resembling (mesogenic[21]) group, in order to enhance the solubility and its interactions with the LC host. This approach is mostly applied to molecules owing their chirality to the presence of a stereogenic centre. A representative example is (*R*)-octan-2-ol **2.1**, which has an extremely low helical twisting power of 0.8 $\mu m^{-1}$ in LC host MBBA (vide supra), probably due to its lack of structural similarity.[22] Functionalization with a group resembling MBBA improved the helical twisting power to 19.4 $\mu m^{-1}$ (Figure 2.10).

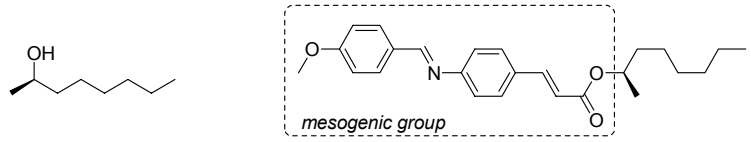


**2.1** $\beta_M$ = 0.8 μm$^{-1}$ (MBBA) **2.2** $\beta_M$ = 19.4 μm$^{-1}$ (MBBA)

**Figure 2.10** Functionalization of a chiral alcohol with a mesogenic group.

A similar procedure was applied in the development of imine-based dopants.[23] Where (*R*)-phenylethylamine **2.3** has an immeasurably small helical twisting power, functionalization with a mesogenic group afforded dopants with helical twisting powers ranging from 17.1 μm$^{-1}$ in phenylbenzoate LC host **2.5** to 43.2 μm$^{-1}$ in biphenyl LC host K15 (Figure 2.11 and Table 2.1). The same principle holds for mesogenic amide functionalization of chiral amines, as the helical twisting powers in cyanobicyclohexyl LC host ZLI-1695 are vastly improved by attaching an alkylbicyclohexyl group to the amine moiety (Figure 2.12).[24] Interestingly, in the same paper an anthraquinone functionalization of chiral amines is described that produces even higher cholesteric induction, although the structural similarity between the anthraquinone and the mesogenic host is not that obvious. In this class of compounds an intramolecular hydrogen bond between the amine and the anthraquinone carbonyl reduces the number of different chiral conformers. According to the authors, this conformational 'locking' is partly responsible for the high helical twisting powers, as the possible conformers all have different helical twisting powers and apparently the ones with a high $\beta$ value are in excess.[24]

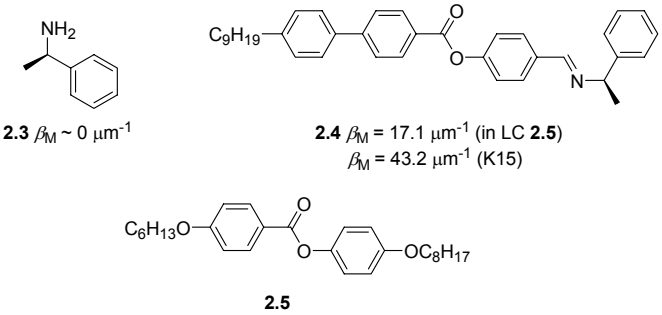


**2.3** $\beta_M$ ~ 0 μm$^{-1}$ **2.4** $\beta_M$ = 17.1 μm$^{-1}$ (in LC **2.5**)
$\beta_M$ = 43.2 μm$^{-1}$ (K15)

**2.5**

**Figure 2.11** Functionalization of a chiral amine with a mesogenic group.

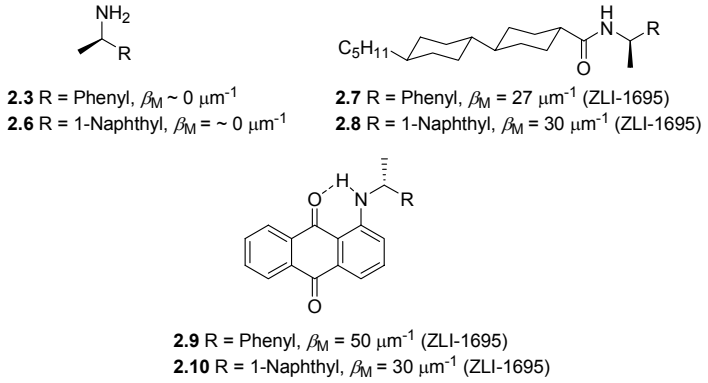


**2.3** R = Phenyl, $\beta_M$ ~ 0 μm$^{-1}$
**2.6** R = 1-Naphthyl, $\beta_M$ = ~ 0 μm$^{-1}$

**2.7** R = Phenyl, $\beta_M$ = 27 μm$^{-1}$ (ZLI-1695)
**2.8** R = 1-Naphthyl, $\beta_M$ = 30 μm$^{-1}$ (ZLI-1695)

**2.9** R = Phenyl, $\beta_M$ = 50 μm$^{-1}$ (ZLI-1695)
**2.10** R = 1-Naphthyl, $\beta_M$ = 30 μm$^{-1}$ (ZLI-1695)

**Figure 2.12** Mesogenic functionalization of chiral amines with bicyclohexyl and anthraquinone moieties.

Overall, the mesogenic functionalization method has not been not particularly successful, as only a few dopants with reasonably high helical twisting powers have been reported.[23-25] However, due to the ease of mesogenic functionalization, some interesting analytical techniques based on this principle have been developed. Rinaldi and coworkers reported that amine **2.3** when dissolved in MBBA undergoes a transimination with the LC host, yielding **2.11** with a helical twisting power of 17.1 μm$^{-1}$ (Figure 2.13).[26] Because of this much higher helical twisting power, a cholesteric phase with a small pitch is easily generated upon doping MBBA with a small amount of **2.3**. As a result of the large supramolecular chirality in this system, liquid crystal induced circular dichroism (LC-ICD) is readily observed, where the sign of the CD is dependent on the absolute configuration of **2.3**. This technique was later expanded to absolute configuration determinations for other amines and amino alcohols, although in these cases no helical twisting powers were reported.[27]

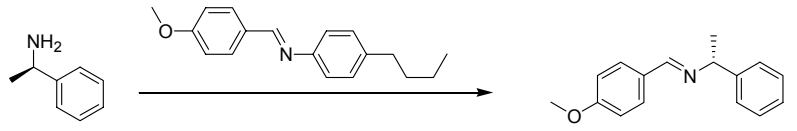


**2.3** $\beta_M$ ~ 0 μm$^{-1}$ **2.11** $\beta_M$ = 17.1 μm$^{-1}$ (MBBA)

**Figure 2.13** Transimination of LC material MBBA with chiral amine **2.3**.

A related approach was taken in 2001 by Feringa and van Delden, who reported the mesogenic functionalization of simple chiral amines and alcohols, leading to LC dopants with $\beta_M$ ranging from 21.1 to 36.7 μm$^{-1}$ in biphenyl dopant E7 (Figure 2.14).[25,28] These high helical twisting powers allowed the generation of colored LC films using the principle described in Section 2.2.4. As the color of

these films is dependent on the enantiomeric excess of the dopants via equations 2.2 and 2.4, this method allowed the evaluation of the enantiomeric excess of simple chiral compounds by inspection of the color after mesogenic derivatization and doping in a nematic LC. Based on this principle, a color test for enantiomeric excess determination of enantioselective reactions was developed, which is described in Chapter 3 of this thesis.[29]

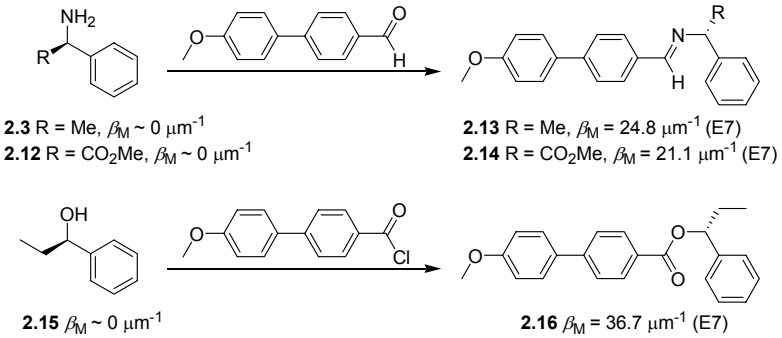


**Figure 2.14** Mesogenic functionalization of chiral amines and alcohols for LC-based color test.

### *2.4.1.2 Chiral coordination complexes*

Coordination complexes owing their chirality either to a chiral ligand or a chiral metal center can be highly effective dopants for induction of cholesteric mesophases. Helical twisting powers up to 180 $\mu m^{-1}$ were found for $C_2$-symmetric ruthenium diketonate complexes **2.17**-**2.19** with $\Delta\Lambda$ chirality at the metal center, with the cholesteric induction being largely dependent on the ligands and the mesogenic host employed (Figure 2.15).[7,30] The observation that chiral chromium diketonate complex **2.20** also has an enormous helical twisting power ($\beta_M$ = 102 $\mu m^{-1}$ in MBBA) shows that mesogenic functionalization as described in the previous section is not essential for this type of dopants, although mesogenic ligands can have a distinct effect on the cholesteric behavior and the solubility of the complex.[31,32] The sign of the cholesteric induction for the ruthenium complexes inversed going from complex **2.17** to complex **2.18**, while the configuration of the metal center remained the same.

The interaction of a chiral dopant with an LC host can also be improved by metal coordination, as was shown for chiral tripyridylamine-based ligands **2.21** and **2.22** (Figure 2.16). Without a metal present, $\beta_M$ values do not exceed 2.2 $\mu m^{-1}$ (**2.22** in MBBA), whereas complexation to Cu(I) or Cu(II) yielded dopants

with greatly enhanced helical twisting powers, up to 98 $\mu m^{-1}$ for **2.21**·$Cu^{II}(ClO_4)(PF_6)$. This effect was attributed to a reduced conformational flexibility of the ligand and a propeller-like shape of the coordination complex.[33]

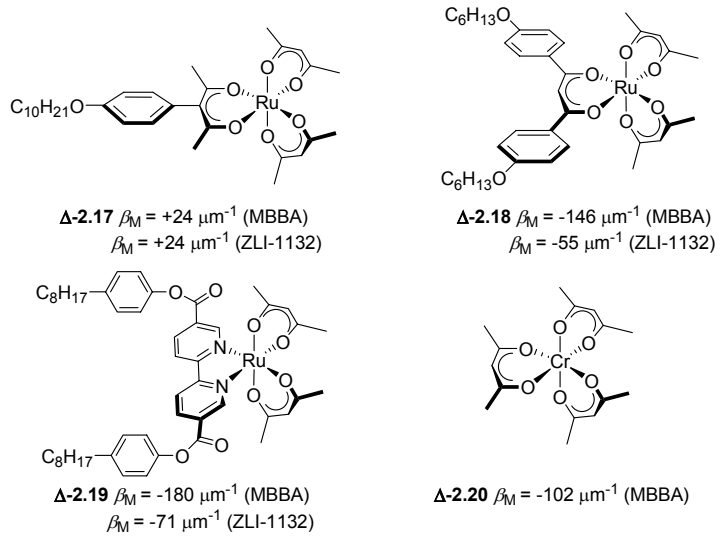


**Δ-2.17** $\beta_M$ = +24 $\mu m^{-1}$ (MBBA)
$\beta_M$ = +24 $\mu m^{-1}$ (ZLI-1132)

**Δ-2.18** $\beta_M$ = -146 $\mu m^{-1}$ (MBBA)
$\beta_M$ = -55 $\mu m^{-1}$ (ZLI-1132)

**Δ-2.19** $\beta_M$ = -180 $\mu m^{-1}$ (MBBA)
$\beta_M$ = -71 $\mu m^{-1}$ (ZLI-1132)

**Δ-2.20** $\beta_M$ = -102 $\mu m^{-1}$ (MBBA)

**Figure 2.15** Chiral coordination complexes with high helical twisting powers.

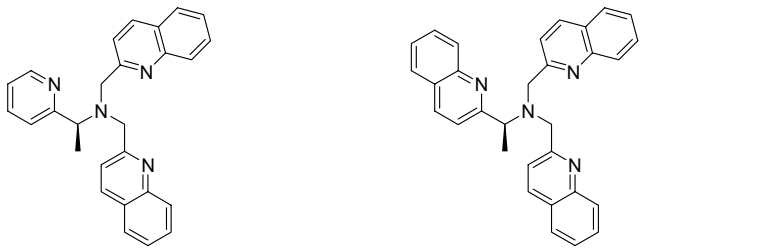

**2.21** $\beta_M$ not determined
**2.21**·Cu(I)$(PF_6)$ $\beta_M$ = -65 $\mu m^{-1}$ (MBBA)
**2.21**·Cu(II)$(ClO_4)(PF_6)$ $\beta_M$ = -98 $\mu m^{-1}$ (MBBA)

**2.22** $\beta_M$ +2.2 $\mu m^{-1}$ (MBBA)
**2.22**·Cu(I)$(PF_6)$ $\beta_M$ = -67 $\mu m^{-1}$ (MBBA)
**2.22**·Cu(II)$(ClO_4)(PF_6)$ $\beta_M$ = -23.7 $\mu m^{-1}$ (MBBA)

**Figure 2.16** Enhancement of helical twisting power by metal coordination.

### *2.4.1.3 Vic-diols and related compounds*

The combination of reasonable backbone rigidity and strategic placement of aryl substituents is generally assumed to afford efficient cholesteric induction.[19] 1,2-diol-based compounds like TADDOLs and 4,5-diaryl-1,3-dioxolanes possess

both these requirements and consequently constitute one of the most effective dopant classes known today (Figure 2.17).

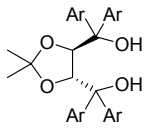


TADDOLs
Ar = phenyl, 2-naphthyl, 9-phenanthryl, etc.
$\beta_M \leq 405\ \mu m^{-1}$

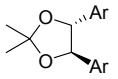


4,5-diaryl-1,3-dioxolanes
Ar = phenyl, 1-naphthyl, mesityl, etc.
$\beta_M \leq 101\ \mu m^{-1}$

**Figure 2.17** TADDOL and 4,5-diaryl-1,3-dioxolanes general structures.

TADDOLs, originally designed as chiral auxiliaries and ligands for asymmetric synthesis, are tartaric acid derivatives with four aryl substituents in a propeller type conformation.[34] In addition to the 1,3-dioxolane structure they also possess a 1,4-diol moiety which participates in intramolecular hydrogen bonding, thereby providing the structures with a fair amount of rigidity. Where the original TADDOL **2.23** with four phenyl substituents already shows an impressive $\beta_M$ of 100 $\mu m^{-1}$ in both LC hosts ZLI-1695 and K15, replacement of the phenyls by 9-phenanthryl groups improves this to 310 $\mu m^{-1}$ and 405 $\mu m^{-1}$, respectively.[35,36,37]

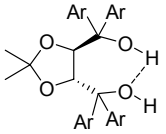


**Table 2.2** Influence of substituents on helical twisting power of TADDOL.

| TADDOL | Ar | $\beta_M$ (ZLI-1695, $\mu m^{-1}$) | $\beta_M$ (K15, $\mu m^{-1}$) |
|---|---|---|---|
| **2.23** | phenyl | +100 | +100 |
| **2.24** | 1-naphthyl | +225 | +230 |
| **2.25** | 2-naphthyl | +180 | +250 |
| **2.26** | 6-HO-2-naphthyl | +200 | +340 |
| **2.27** | 9-phenanthryl | +310 | +405 |
| **2.28** | 4'-biphenyl | +130 | +185 |

All in all, eight TADDOLs with helical twisting powers over 100 $\mu m^{-1}$ were described, differing in aryl and dioxolane bridge substituents (Table 2.2). The

importance of the intramolecular hydrogen bonding of the 1,4-diol moiety was demonstrated by methylation of the hydroxyl groups, which reduced the helical twisting power from 100 $\mu m^{-1}$ (**2.23**) to 55 $\mu m^{-1}$ (**2.29**) (ZLI-1695). Similarly, replacement of the 1,4-diol by a silane bridge lowered $\beta_M$ to 23 $\mu m^{-1}$ (Figure 2.18).

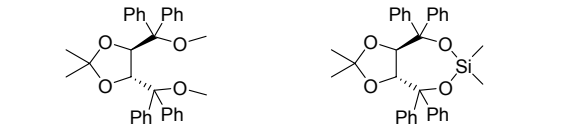


**2.29** $\beta_M$ = +55 $\mu m^{-1}$ (ZLI-1695) **2.30** $\beta_M$ = +23 $\mu m^{-1}$ (ZLI-1695)
$\beta_M$ = +25 $\mu m^{-1}$ (K15)

**Figure 2.18** Influence of bridging substituents on the helical twisting power of tetraphenyl-TADDOL.

An interesting correlation between backbone shape, aryl configuration and cholesteric induction can be observed for 4,5-diaryl-1,3-dioxolanes **2.31** and related oxiranes like **2.39** (Figure 2.20).[38] For 4,5-diaryl-1,3-dioxolanes, two conformations are conceivable, of which the quasi-gauche **2.31a** is preferred due to steric interactions of the aryl substituents with the methyl groups on the dioxolane bridge in the staggered form (**2.31b**) (Figure 2.19).

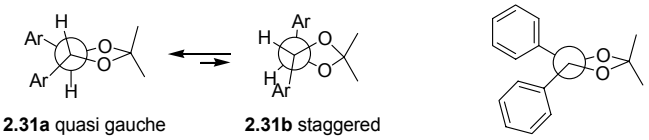


**2.31a** quasi gauche **2.31b** staggered

**Figure 2.19** Conformational equilibrium of 4,5-diaryl-1,3-dioxolanes.

In this quasi-gauche conformation the aryls have to adopt an arrangement nearly perpendicular to the plane of the dioxolane ring, with a resulting helicity of which the sign depends on the configuration of the molecule. Many 4,5-diaryl-1,3-dioxolanes show high helical twisting powers in E7, with the highest $\beta_M$ obtained for dopants with large aryl substituents (Table 2.3). The steric bulk on the aryls is believed to force them into this helical conformation, thus producing an overall configuration of the molecule that is ideal for dopant-LC interactions.

Interestingly, where 4,5-diaryl-1,3-dioxolanes display large cholesteric induction in E7, helical twisting powers in MBBA are always lower (Figure 2.20). As the length of the aromatic array of dioxolane **2.32** is similar to the biphenyl part of E7, but approximately 2 Å shorter than MBBA, π-stacking interactions between these two moieties seem responsible for the magnitude of the cholesteric induction. This conclusion is supported by the finding that chiral diaryloxiranes,

with an aromatic array similar to MBBA in length, have higher helical twisting powers in MBBA than in E7. Based on these findings a model for the interaction between dopant and mesogen molecules was proposed (Figure 2.21).

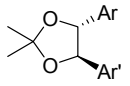


**Table 2.3** Influence of dioxolane substitution on helical twisting power.

| dioxolane | Ar | Ar' | $\beta_M$ (MBBA, $\mu m^{-1}$) | $\beta_M$ (K15, $\mu m^{-1}$) |
|---|---|---|---|---|
| **2.32** | phenyl | phenyl | -5.4 | -17.8 |
| **2.33** | 1-naphthyl | 1-naphthyl | -48.7 | -58.3 |
| **2.34** | 2-naphthyl | 2-naphthyl | -23.1 | -36.1 |
| **2.35** | 1-naphthyl | 2-naphthyl | -20.9 | -26.2 |
| **2.36** | mesityl | mesityl | -59.5 | -101 |
| **2.37** | 4-tolyl | 4-tolyl | -18.2 | -22.3 |
| **2.38** | 4'-biphenyl | 4'-biphenyl | -28.5 | -58 |

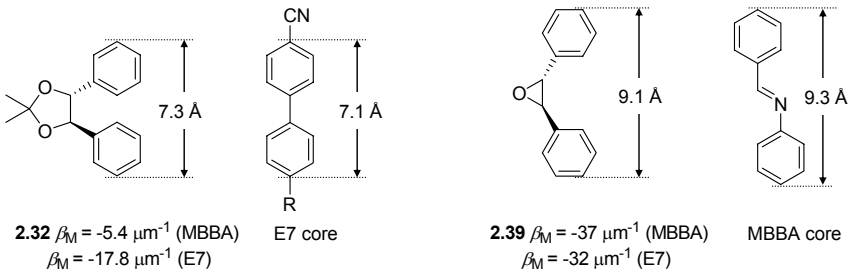


**Figure 2.20** Comparison of aryl-aryl distances in dopants **2.32** and **2.39**, and LC cores of E7 and MBBA. The distances were obtained by computational modeling.

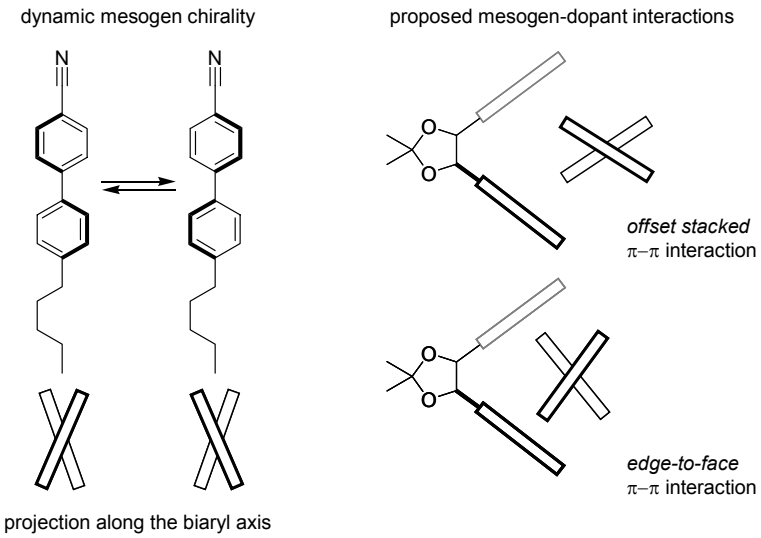


**Figure 2.21** Model for the interactions between 4,5-diaryl-1,3-dioxolanes and biphenyl mesogens. The twisted biaryl core of the mesogen is situated in the aromatic cleft of the dioxolane.

It comprises an aromatic helical cleft on the dopant, capable of interactions with the mesogen, and thereby inducing a preferred helicity in this mesogen. This preferred chirality in the mesogen is then transferred via neighboring mesogens to the bulk LC phase.[19] Although a possible mechanism, it was never confirmed experimentally.

### *2.4.1.4 Atropisomer-based dopants*

By far the most extensively studied class of chiral dopants consists of inherently chiral molecules, like binaphthyls, biphenyls and helicenes (Figure 2.22). These compounds are generally characterized by the absence of stereogenic centers; instead they possess a chiral plane or axis. As a result of their synthetic accessibility and generally high helical twisting powers, they are widely applied in liquid crystal research.

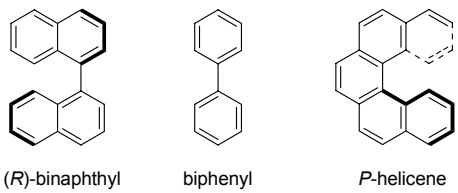


**Figure 2.22** Binaphthyl, biphenyl and helicene core structures.

Optically pure 1,1'-binaphthyl compounds can exist in two conformations, either cisoid or transoid, as the dihedral angle (θ) between the two naphthalene rings is dependent on the substituents at the 2 and 2' positions (Figure 2.23). When these substituents are either covalently linked or capable of intramolecular hydrogen bonding, the cisoid conformation is preferred, whereas the presence of large, unlinked substituents leads to a more favorable transoid conformation. The helical twisting power of 1,1'-binaphthyl compounds is largely dependent on the dihedral angle.[39,40,41]

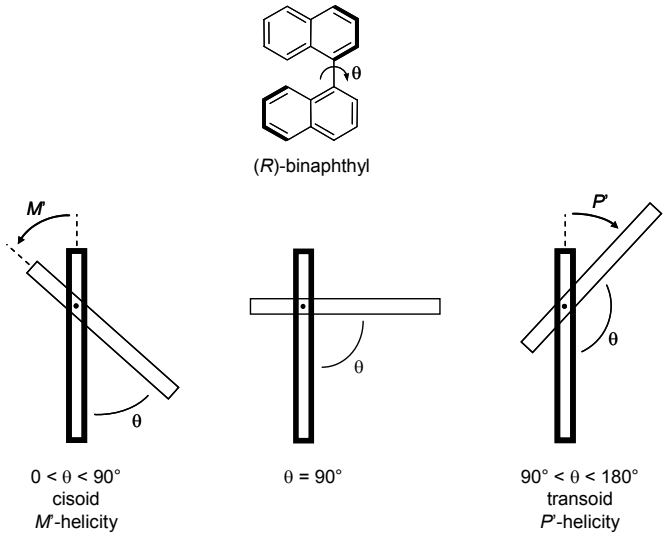


**Figure 2.23** (*R*)-binaphthyl and associated conformers.

Especially cisoid compounds exhibit large cholesteric induction, whereas transoid dopants are usually somewhat less efficient. Lowest helical twisting powers are obtained for compounds with a dihedral angle close to 90°, often found for 1,1'-binaphthyls with small, unlinked substituents at the 2,2' positions. In addition to these features, the sign of the induced cholesteric helix is also dependent on the dihedral angle. For 1,1'-binaphthyls with the same absolute configuration, a cisoid dopant will provide a cholesteric helicity opposite from that obtained using the transoid type. This is explained by the opposite pseudo helicities of these two conformations, as defined in Figure 2.23.[42] An *S*-cisoid dopant will have pseudo-*P* helicity, leading to *P* cholesterics, whereas an *S*-transoid dopant has pseudo-*M* helicity and will induce an *M* cholesteric helix. These effects are clearly observed in 1,1'-binaphthyl-2,2'-diol (BINOL) derivatives (Figure 2.24). The $\beta_M$ of +32 $\mu m^{-1}$ (K15) for (*S*)-BINOL **2.40** is the

result of intramolecular hydrogen bonding between the two hydroxyl moieties, leading to a cisoid conformation.[39] Bridged BINOL derivatives have even higher helical twisting powers, up to +85 $\mu m^{-1}$ (K15) for (*S*)-**2.41**.[43] However, methylation of both hydroxyl substituents reduces the helical twisting power to +1.5 $\mu m^{-1}$ ((*S*)-**2.44**, K15), indicating a dihedral angle close to 90°, or an equal population of cisoid and transoid conformation due to the high flexibility of the structure of **2.44**. Substitution of the hydroxyl group by large isopropoxy substituents enhances the steric hindrance which results in a more effective cholesteric induction ($\beta_M$ = -8.2 $\mu m^{-1}$, K15), but reversal of sign, indicative of a transoid conformation.[44]

Using linear dichroism (LD) the orientation of dopants **2.43** and **2.44** in nematic LC ZLI-1167 was determined, where it was found that the twofold symmetry axes of these molecules are aligned perpendicular to the nematic director.[39,43] Similar to the 1,2-diols described in Section 2.4.1.3, dopants **2.40**-**2.43** perform better in biphenyl hosts E7 and K15 than in imine-based MBBA. Based on these two observations a model for the interaction of binaphthyl dopants and biphenyl LC hosts was proposed (Figure 2.25). In this model the dopant and a mesogen are associated through π-interactions, with their individual biaryl axes in parallel alignment. Through a mechanism similar to that described in Section 2.4.1.3 , the chirality is then transferred to the bulk mesophase.

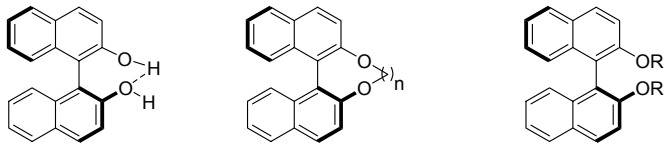


**2.40** $\beta_M$ = + 32 $\mu m^{-1}$ (K15)

**2.41** n=1, $\beta_M$ = + 85 $\mu m^{-1}$ (K15)
**2.42** n=3, $\beta_M$ = + 80 $\mu m^{-1}$ (K15)
**2.43** n=4, $\beta_M$ = + 79 $\mu m^{-1}$ (K15)

**2.44** R = Me, $\beta_M$ = + 1.5 $\mu m^{-1}$ (K15)
**2.45** R = *i*-Pr, $\beta_M$ = - 8.2 $\mu m^{-1}$ (K15)

**Figure 2.24** Helical twisting powers of BINOL derivatives depending on their substitution pattern.

In general, the magnitude and sign of cholesteric induction in biphenyl mesogens by BINOL-based dopants is in accordance with the model described above.[45,46,47] Depending on the substitution around the naphthalene rings, open chain dopants usually possess helical twisting powers up to 50 $\mu m^{-1}$, whereas in their bridged analogues these values can go up to 130 $\mu m^{-1}$. Structurally similar 4,4'-biphenanthryls and helicenes show comparable behavior.[48] An interesting exception is BINOL dimer **2.46**, reported by Diederich and Spada, which has remarkably high helical twisting powers, both in E7 ($\beta_M$ = -242.3 $\mu m^{-1}$) and MBBA ($\beta_M$ = -239.5 $\mu m^{-1}$) (Figure 2.26).[47] As these values are much higher than

can be expected from simply adding two BINOL monomers with similar substitution patterns, the cholesteric induction is thought to proceed via a different, yet unknown, mechanism.

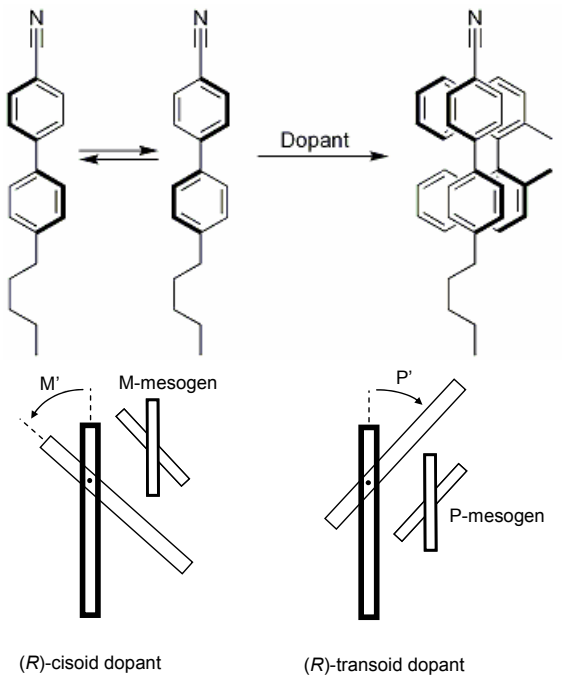


**Figure 2.25** Proposed model for the transfer of chirality from the binaphthyl dopant to the mesogens.

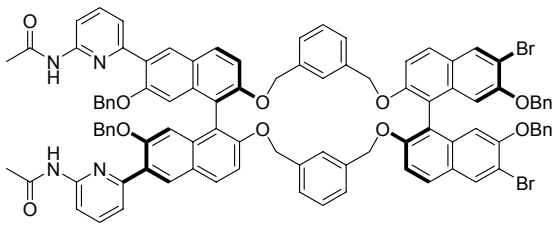


**2.46** $\beta_M$ = -239.5 $\mu m^{-1}$ (MBBA)
$\beta_M$ = -242.3 $\mu m^{-1}$ (E7)

**Figure 2.26** A BINOL dimer with a high helical twisting power.

Chiral biphenyls do not fit the model with great uniformity, despite the structural similarity to binaphthyls (Figure 2.27).[49,50] Especially 4,4'-substituted biphenyls tend to induce cholesteric LC phases with helicities opposite to those predicted by the model.[39] This behavior could be the result of a different dopant orientation with respect to the nematic director, which was supported by calculations on the dopant order parameter.[51]

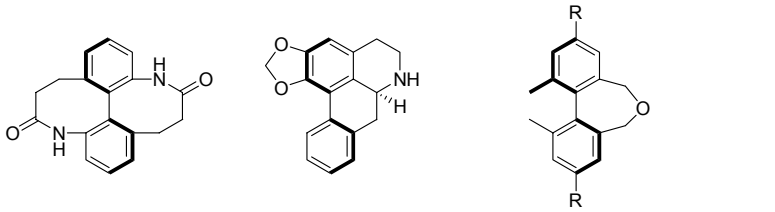


**2.47** $\beta_M$ = +58 $\mu m^{-1}$ (E7) **2.48** $\beta_M$ = +24 $\mu m^{-1}$ (E7) **2.49** R = H, $\beta_M$ ~ 0 $\mu m^{-1}$ (E7)
**2.50** R = OMe, $\beta_M$ = -11.4 $\mu m^{-1}$ (E7)
**2.51** R = Br, $\beta_M$ = -19.3 $\mu m^{-1}$ (K15)
**2.52** R = $NO_2$, $\beta_M$ = -20.3 $\mu m^{-1}$ (K15)

**Figure 2.27** Some chiral biphenyl derivatives and associated helical twisting powers.

A study on chiral heptalene derivatives revealed a comparable dependence of the helical twisting power on the orientation of the dopant.[52] Heptalenes are intrinsically dissymmetric molecules with a highly twisted $C_2$ or nearly $C_2$ symmetric structure, without the presence of stereogenic centers.[53] The propeller like structure has the intriguing feature that, for any given conformation, the heptalene skeleton has opposite helicities in the x and y directions (Figure 2.28).

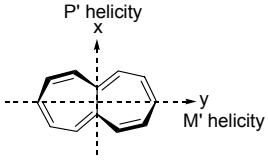


**Figure 2.28** Heptalene general structure and double helicity; the x-axis helicity is used in absolute configuration description of the molecules.

Heptalenes of the same absolute configuration were found to show opposite helical twisting powers depending on the substituents around the rings (Figure 2.28).[52] The cholesteric induction by derivative *P*-**2.53** is reflected in a moderate +23 $\mu m^{-1}$ (E7) whereas *P*-**2.54** shows a $\beta_M$ of -27 $\mu m^{-1}$ (Figure 2.29).

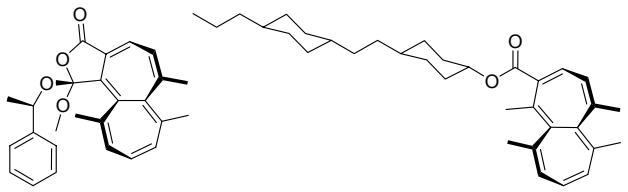

**2.53** $\beta_M$ = + 23 $\mu m^{-1}$ (E7) **2.54** $\beta_M$ = -27 $\mu m^{-1}$ (E7)

**Figure 2.29** Opposite helical twisting powers of functionalized heptalenes depending on the substitution pattern.

*P*-**2.53** is oriented with its x axis parallel to the nematic director, as was determined by linear dichroism. *P*-**2.54** has its y-axis parallel to the director, showing that the sign of the cholesteric induction is governed by the axis helicity in agreement with the model described above.

The concept of mesogenic functionalization has also been applied to chiral biphenyl and binaphthyl derivatives, with effects similar to those observed for molecules with central chirality (Section 2.4.1.1). Moderate cholesteric induction was reported with mesogenically functionalized biphenyls, with a pronounced influence of the way in which the mesogenic group is tethered to the biphenyl (Figure 2.30).[51,54,55] Mesogenic functionalization of BINOL proved quite fruitful, providing a $\beta_M$ of around 200 $\mu m^{-1}$ for **2.58** (Figure 2.31).[56]

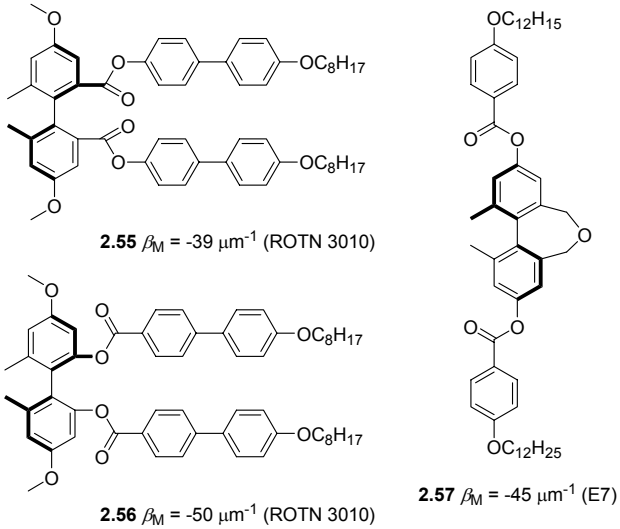

**2.55** $\beta_M$ = -39 $\mu m^{-1}$ (ROTN 3010)

**2.56** $\beta_M$ = -50 $\mu m^{-1}$ (ROTN 3010)

**2.57** $\beta_M$ = -45 $\mu m^{-1}$ (E7)

**Figure 2.30** Mesogenic functionalization of chiral biphenyls.[55]

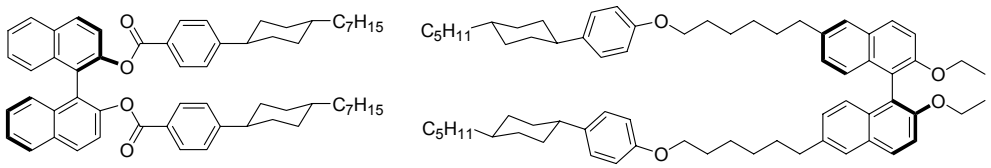


**2.58** $\beta_M$ ~ 200 μm$^{-1}$ (ROTN 404) **2.59** $\beta_M$ not determined

**Figure 2.31** Mesogenic functionalization of chiral BINOL derivatives.[56]

Akagi and coworkers reported a Ziegler-Natta type acetylene polymerization *in* a cholesteric film doped with BINOL derivative **2.59,** yielding helical polyacetylene.[57,58,59] In this system, the asymmetric nature of the polymerization is dictated by the cholesteric helicity and not directly by any chiral ligand on the catalyst. No helical twisting power was reported for this dopant, although by comparison to other systems,[45,59] it is not expected to be higher than 100 μm$^{-1}$, and probably considerably lower. It is not entirely clear why such a complicated molecule has to be applied, when much simpler and more efficient dopants are readily available (vide supra).

Results comparable to the BINOL mesogenic functionalization were obtained for helicene-based hexahydrobenzo[c]phenantrenes (Figure 2.32).[60] Without mesogenic groups helical twisting powers remained low, whereas the incorporation of 4'-alkylbiphenyl groups improved the cholesteric induction to an impressive 147.9 μm$^{-1}$ (MBBA).

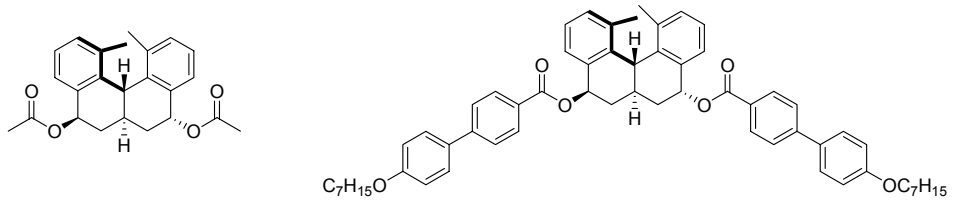


**2.60** $\beta_M$ = 7.8 μm$^{-1}$ (MBBA) **2.61** $\beta_M$ = 147.9 μm$^{-1}$ (MBBA)

**Figure 2.32** Mesogenic functionalization of helicene derivatives.

### 2.4.2 Bistable Dopants for Photocontrol of Liquid Crystalline Phases

The incorporation of bistable ('switchable') moieties in liquid crystal dopants offers the possibility of controlling the supramolecular chirality of cholesteric liquid crystalline phases using external stimuli (Figure 2.33).[20] Furthermore, as the helical pitch and sign of helicity are a direct result of the state of the dopant incorporated, the macroscopic properties of the cholesteric LC can be applied

for non-destructive read-out of the switch state (vide infra), and amplification of its chirality. Especially photochemical switching of cholesteric phases might lead to materials with potential applications in all-optical devices, enhanced speed of data processing and the possibility of controlling the selective reflection and transmission of light.

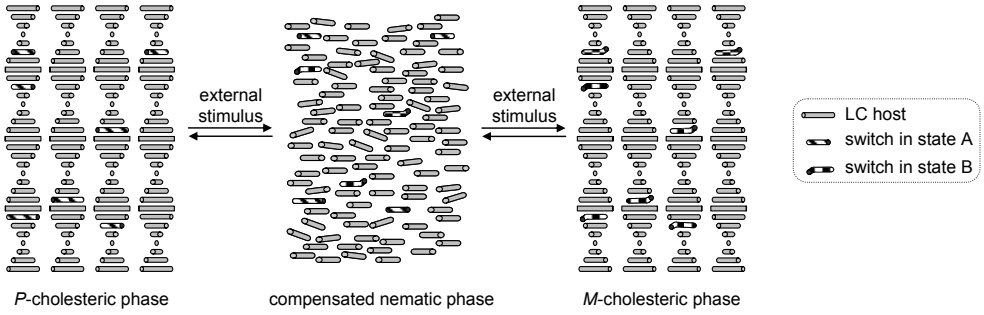


**Figure 2.33** Schematic representation of the switching of the chirality of a doped cholesteric liquid crystal.

*2.4.2.1 Switches*

In recent years, much attention has been paid to the development of molecular machinery, for use in the *bottom-up* approach in nanotechnology.[61] An essential part in this nanotechnology toolbox is a simple switch that can differentiate between two states, and as such provides the molecular equivalent of the electronic *on* and *off* switch (Figure 2.34).

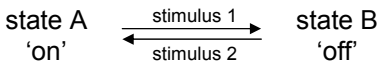


**Figure 2.34** Schematic representation of a bistable switch.

For this purpose many different molecular systems have been developed, including catenanes, rotaxanes, azobenzenes, overcrowded alkenes, fulgides, diarylethenes, and spiropyrans.[62] Some of these systems are chiral and as such can, in theory, be applied as bistable dopants for switching between different cholesteric states. Although in principle a variety of external stimuli, such as pH, solvent, pressure, magnetic or electric fields, heat, light and chemical reactions can be applied to achieve switching,[63] generally only heat and light are used for switching in liquid crystal systems, due to their non-destructive nature. Especially light offers enormous advantages over other stimuli, as it can be used at selected wavelengths, distinct polarizations and intensities. Furthermore it

offers the possibility of using lasers and masks, for accurate irradiation of defined areas. As a result of these features, practically all switches designed for use in an LC matrix are optical switches, i.e. they experience a change in certain properties upon irradiation with a specific wavelength of light. Three different chiral optical switches can be distinguished (Figure 2.35).

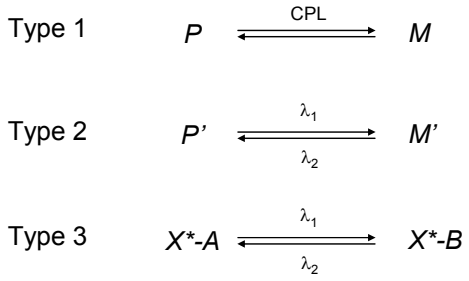


**Figure 2.35** Schematic representation of different types of chiral switches. *P* and *M* represent molecular helicities, *X** represents a chiral auxiliary unit in the molecule.

In Type 1 the switching takes place between enantiomers, in which case irradiation with unpolarized light leads to racemization of the switch, due to the equal absorption of light as a result of the enantiomeric relationship of the two states. Therefore, circular polarized light is needed to switch selectively from one state to the other. Type 2 describes switching of pseudoenantiomers, where the chiral properties of the switch are inversed upon switching, but the two states do not have an enantiomeric relationship. Irradiation with unpolarized light can then lead to selective interconversion between the usually diastereomeric states. In Type 3 switches, comprising a switching unit and a chiral auxiliary unit, the chirality of the system does not change so dramatically, for instance because the switching moiety is situated more remote from the chiral unit in the molecule. However, switching does result in conformational change and as a result of that influences the chiral properties of the entire molecule.

### *2.4.2.2 Type 3 switchable dopants*

#### *2.4.2.2.1 Azobenzene-based switchable dopants*

Azobenzenes can undergo a reversible *trans-cis* (or *E-Z*) isomerization upon irradiation with UV/VIS light, resulting in large conformational and polarization changes in the molecule. The *trans* form has a rod-like structure and as such can stabilize calamitic liquid crystals, whereas the *cis* form is bent and generally destabilizes the LC superstructure by generating disorder in the aligned systems (Figure 2.36). This principle has been applied in photochemical orientation of

nematic films,[20] pitch change in cholesterics[20,64] and phase transitions from nematic to isotropic states.[65] The first dopant ever to effect a change in cholesteric pitch upon irradiation was an achiral dopant containing an azobenzene core.[66] Even today the azobenzene moiety is the most frequently applied bistable group in liquid crystal research. It is easily synthesized and generally shows good compatibility with the LC phase, especially in the *trans* form. Moreover, due to the large difference in structure the helical twisting powers of *trans* and *cis* isomers are usually quite different, which allows efficient switching of the cholesteric pitch.

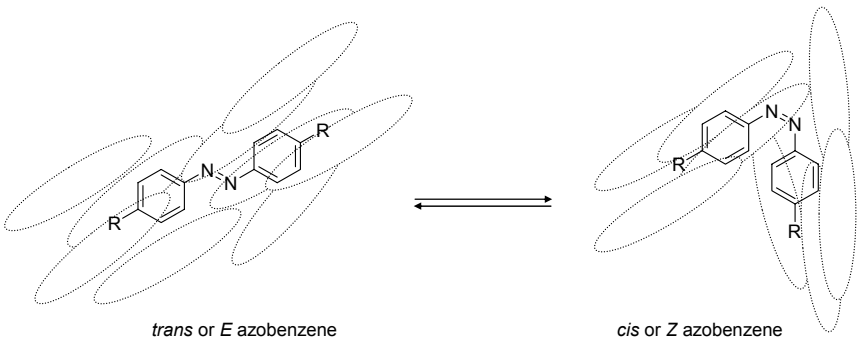


**Figure 2.36** Destabilization of liquid crystalline order by *trans* to *cis* isomerization of an azobenzene dopant.

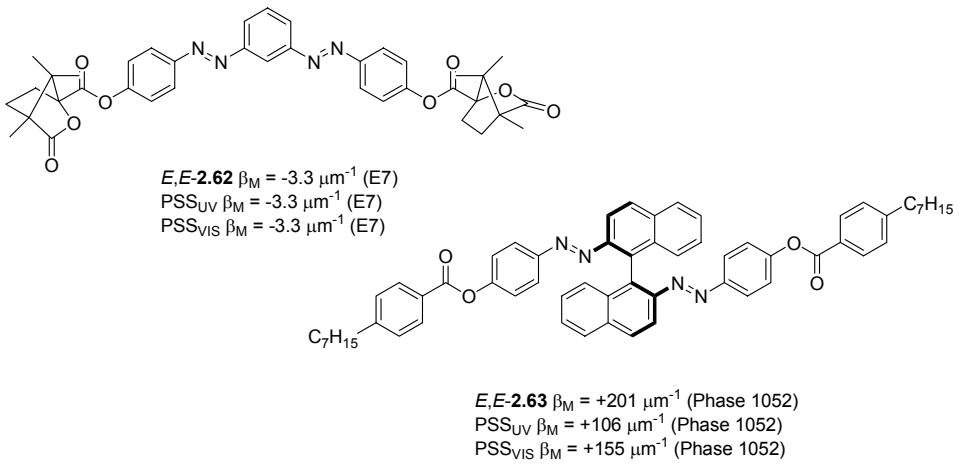


**Figure 2.37** Azobenzene-based dopants and associated helical twisting powers.

Similar to the shape persistent dopants described in Section 2.4.1, the helical twisting powers of chiral azobenzene-based dopants are largely dependent on the nature of the chiral group in the molecule. In general, azobenzenes with an atropisomeric moiety show much more efficient chiral induction than azobenzenes possessing central chirality (Figure 2.37). For the latter type of compounds, the highest helical twisting powers reported are around 15 $\mu m^{-1}$,[67] whereas binaphthyl-based azobenzenes can have $\beta_M$ over 200 $\mu m^{-1}$.[68,69,70] The *trans* isomers normally show more efficient cholesteric induction than the *cis* form, in accordance with the model presented in Figure 2.36. However, when substituted at the 2,2'- and 3,3'-positions, the *cis* isomers possess a more rod-like character and the structural modification is associated with higher helical twisting powers (Figure 2.38).[71]

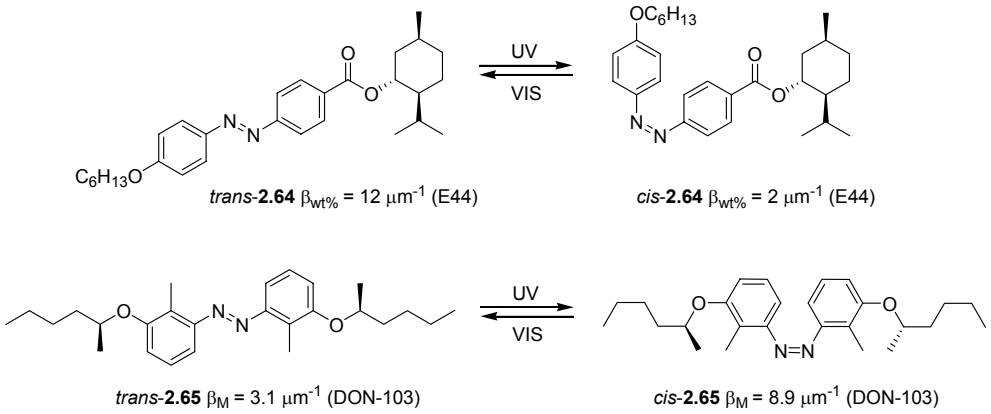


**Figure 2.38** 4,4'- vs. 3,3'-Disubstituted chiral azobenzenes as bistable dopants.[72]

As the helical twisting powers of these azobenzenes are generally low, selective color reflection of the LC film with these photobistable dopants as guests (see Section 2.2.4) and manipulation of this color by optical switching is practically impossible. However, high compatibility with calamitic mesogens made the use of chiral non-photo addressable co-dopants of enhanced compatibility and helical twisting power feasible, resulting in efficient switching of colored cholesteric films (Figure 2.39).[20,67c,67e,73] The helical twisting power of azobenzene switches was considerably enhanced by incorporation of axially chiral binaphthyl moieties. Especially binaphthyldiamine-based switches **2.63** (Figure 2.37), **2.68** and **2.69** (Figure 2.40), developed by Gottarelli and Spada, constitute a powerful system for optical switching of the cholesteric pitch, as the high helical twisting powers allow for color generation and switching without added chiral co-dopants.[69] Furthermore, UV irradiation of an LC film doped with switch **2.69** ($\beta_M$ = +37 $\mu m^{-1}$, $PSS_{VIS}$, in ZLI-2359) leads to a cholesteric

phase of opposite helicity ($\beta_M$ = -31 μm$^{-1}$, $PSS_{UV}$), a phenomenon that is rarely observed to such degree for Type 3 switches.[74,75]

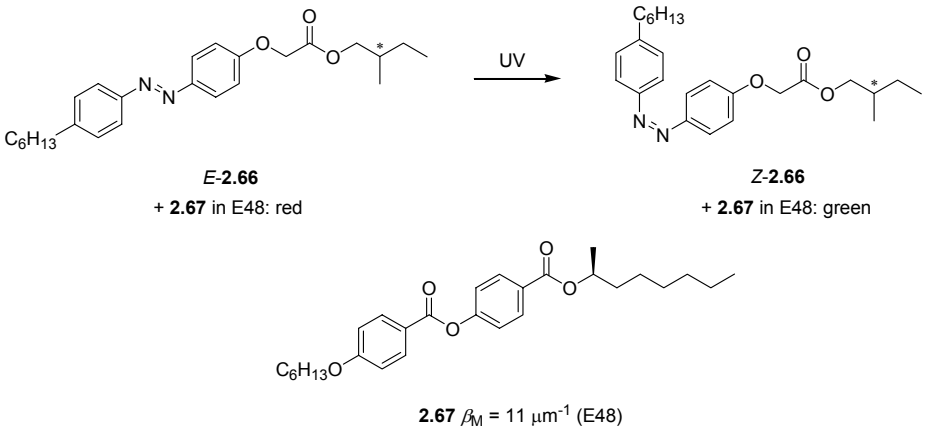


**Figure 2.39** Photochemical modulation of the color of a liquid crystalline film using a chiral co-dopant. The exact helical twisting power of **2.66** is unknown, but too low to generate a reflective LC film in E48 on its own. Chiral co-dopant **2.67** has a moderate helical twisting power but a high compatibility with the LC host, allowing doping of high concentrations leading to colored LC films.[73a,76]

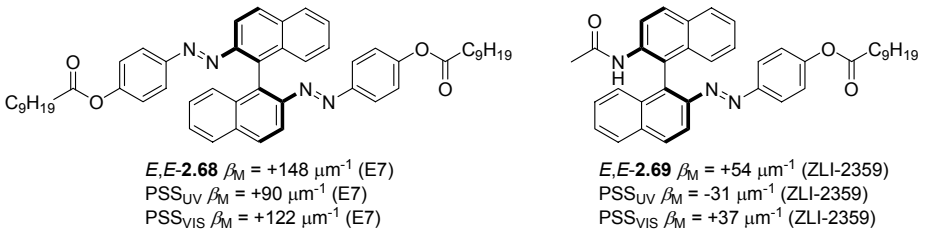


**Figure 2.40** Binaphthalene-based azobenzene switches showing efficient cholesteric induction.

*2.4.2.2.2Olefin-based switchable dopants*

The same *trans/cis* isomerization is also used for switching of chiral cyclohexane derivatives with an exocyclic olefinic double bond.[77] Menthone derivatives showing high helical twisting powers and efficient cholesteric pitch switching were reported,[78] and later these compounds were also used for light induced color change of cholesteric copolymers (Figure 2.41).[79]

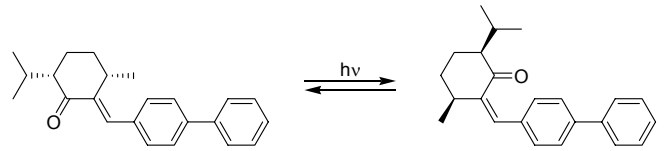


*trans*-**2.70** $\beta_M$ = -41 μm$^{-1}$ (MBBA)
$\beta_M$ = -36 μm$^{-1}$ (E7)

*cis*-**2.70** $\beta_M$ = +8 μm$^{-1}$ (MBBA)
$\beta_M$ = -1 μm$^{-1}$ (E7)

**Figure 2.41** Menthone-based switchable dopants.

*2.4.2.2.3Diaryl ethenes*

Photochromic diaryl ethenes undergo a reversible 6π electron cyclization upon irradiation, leading to distinct changes in structure and electronic configuration of the molecule.[80] This switching unit has been applied for reversible cholesteric to nematic transitions and manipulation of the cholesteric pitch.[81,82] The cholesteric to nematic transitions were made possible because in all described cases either the closed or the open form of the switch has an extremely low helical twisting power (Figure 2.42). Overall, the cholesteric induction by this type of switches is not very efficient.

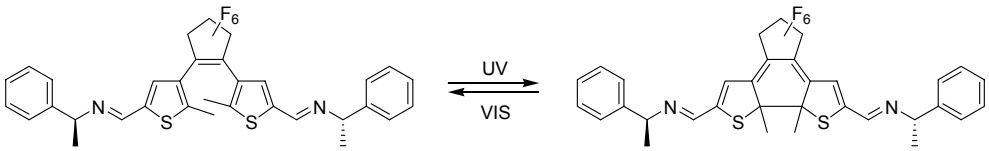


open-**2.71** $\beta_M$ = 13 μm$^{-1}$ (ZLI-389)

closed-**2.71** $\beta_M$ ~ 0 μm$^{-1}$ (ZLI-389)

**Figure 2.42** Diarylethene-based switchable dopants.

*2.4.2.2.4Fulgides*

A similar reversible 6π electron cyclization is used for switching fulgides.[83] The incorporation of a chiral binaphthol moiety in the switch resulted in a bistable system with an enormous difference in helical twisting power between the open and closed forms of the switch (Figure 2.43).[84] The open form of chiral fulgide **2.72** has a $\beta_M$ of -28.0 μm$^{-1}$ in K15, whereas ringclosure leads to an impressive $\beta_M$ of -175.3 μm$^{-1}$. This allows photoswitching between cholesteric phases with a long and a short pitch, respectively, using very small amounts of dopant. However, it does not result in a change in sign of the cholesteric helicity. This shortcoming was circumvented by addition of non-switchable chiral dopant **2.41** showing opposite helical twisting power (+85 μm$^{-1}$, see Section 2.4.1.4),

resulting in reversible switching between a positive and negative cholesteric phase.[84b]

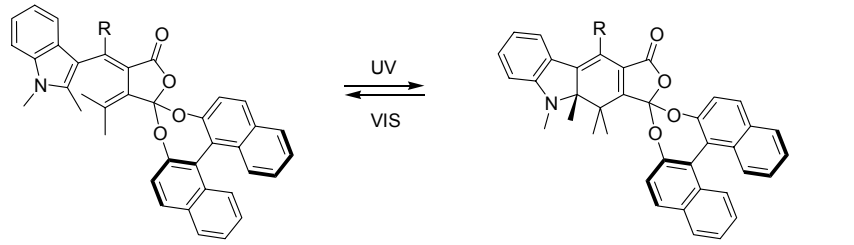


open-**2.72** R = *i*-Pr, $\beta_M$ = -23 μm$^{-1}$ (K15)
open-**2.73** R = *n*-Pr, $\beta_M$ = -28 μm$^{-1}$ (K15)

closed-**2.72** R = *i*-Pr, $\beta_M$ = -175 μm$^{-1}$ (K15)
closed-**2.73** R = *n*-Pr, $\beta_M$ = -175.3 μm$^{-1}$ (K15)

**Figure 2.43** Fulgide-based switchable dopants.

### *2.4.2.3 Type 2 switchable dopants*

#### *2.4.2.3.1 Overcrowded alkenes*

As a result of the pseudoenantiomeric relationship[85] between the two switch states, Type 2 switches are much more likely to show inversion of the cholesteric helix sign upon switching than Type 3 switches. This principle was first shown for the overcrowded alkene-based switches developed in this laboratory.[86,87] The inherently dissymmetric alkene *cis*-**2.74** has an *P* chirality, which, upon irradiation with UV light, is converted to its *M-trans* isomer (Figure 2.44).

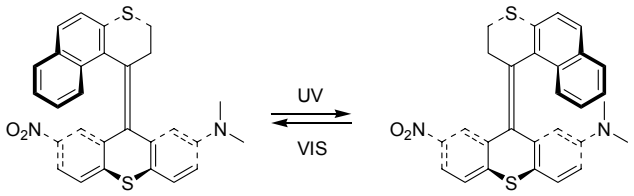


*P-cis*-**2.74** $\beta_M$ = +5.9 μm$^{-1}$ (M15)
$PSS_{435nm}$ = 88:12 (*trans*:*cis*)
*positive cholesteric helicity*

*M-trans*-**2.74** $\beta_M$ = -9.6 μm$^{-1}$ (M15)
$PSS_{313nm}$ = 75:25 (*cis*:*trans*)
*negative cholesteric helicity*

**Figure 2.44** Overcrowded alkene-based molecular switch **2.74** and its influence on a liquid crystalline host.

The pseudoenantiomeric relationship of these two isomers is clearly reflected in their CD spectra. Doping of LC host M15 with *P-cis*-**2.74** transformed this

nematic phase to a cholesteric phase with positive helicity ($\beta_{M,cis}$ = +5.9 μm$^{-1}$).[88] Irradiation with UV light then led to a photostationary state consisting of 75% *M-trans*-**2.74** and 25% *P-cis*-**2.74** and an overall negative cholesteric helicity. The *M-trans* switch has a helical twisting power of -9.6 μm$^{-1}$. Subsequent irradiation with 465 nm light led to a photostationary state made up of 88% *P-cis* and 12% *M-trans*, and consequently a positive helical pitch. Similar results were obtained in other liquid crystalline hosts and with structural variants of switch **2.74**.[89,90,91] Overall, helical twisting powers of this type of switches are not very high, but cholesteric helix inversion takes place quite efficiently and with nearly equal magnitude as a result of the pseudoenantiomeric relationship of the switch states. Light-driven unidirectional molecular motors were also used as chiral guests in LC host materials. For the first generation of the overcrowded alkene-based molecular motors, also developed in this laboratory,[92] the behavior mentioned above is inversed compared to the switches; $\beta_M$ of the stable *P*,*P-trans* form is +109 μm$^{-1}$ (M15), but generation of a cholesteric helix with an opposite sign of similar pitch is impossible, as only the *M*,*M-trans* form possesses a minor negative helical twisting power ($\beta_M$ = -26 μm$^{-1}$, M15).[90,93] As a result of the high helical twisting power of the *P*,*P-trans* form, colored liquid crystalline films are easily generated using this dopant. Photochemical and thermal isomerization of the motor leads to irreversible color change in the LC film. This system will be further discussed in Chapters 6 and 7 of this thesis.

#### *2.4.2.4 Type 1 switchable dopants*

Bistable switches with an enantiomeric relationship between the switch states can be interconverted using circularly polarized light. Furthermore, irradiation of a racemic Type 1 switch with CPL of one handedness can lead to partial photoresolution. As the two enantiomers absorb left- or right-handed CPL differently, one enantiomer is excited preferentially, leading to racemization. The other enantiomer is affected less and will accumulate until an equilibrium or photostationary state is reached. The enantiomeric excess of this photostationary state at a certain wavelength of irradiation depends on the Kuhn anisotropy factor $g_\lambda$, defined as the ratio of the circular dichroism ($\Delta\varepsilon$) and the extinction coefficient ($\varepsilon$) (eq. 2.5).

$$ee_{PSS} = \frac{g_\lambda}{2} = \frac{\Delta\varepsilon}{2\varepsilon} \qquad \textbf{eq. 2.5}$$

As $g$-values normally do not exceed 0.01, CPL photoresolution seldom leads to enantiomeric excesses over 0.5%.[94] Such *ee* values can be difficult to determine using conventional methods. However, as the conversion from nematic to

cholesteric is essentially thresholdless, these *ee*s are theoretically high enough to trigger a nematic to cholesteric transition. The *ee* can then be determined from the cholesteric pitch via equation 2.5. Likewise, using this system the helicity of a cholesteric phase can be controlled using only the chiral information in the circularly polarized light. Finally, a cholesteric to nematic transition can be caused by irradiation with unpolarized or linearly polarized light, leading to racemization of the chiral switch.

#### 2.4.2.4.1 Overcrowded alkenes

The concept described above was first proven using inherently dissymmetric overcrowded alkene **2.75** (Figure 2.45).[95,87] Irradiation of this racemic Type 1 switch with *l*-CPL (313 nm) led to *M*-**2.75** with 0.07% *ee*. When this irradiation was carried out in a nematic LC host[88] (20 wt% **2.75** in M15) a cholesteric phase was generated, which disappeared again upon irradiation with linearly polarized light. Irradiation with *r*-CPL resulted in a cholesteric phase of opposite handedness.

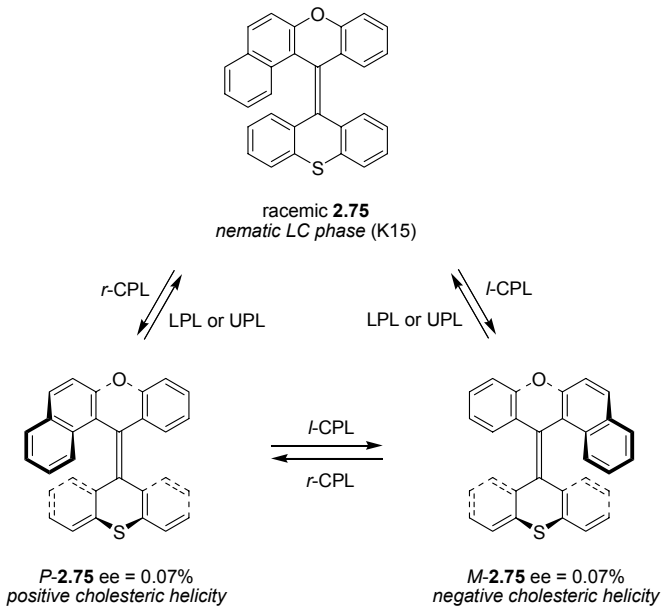


**Figure 2.45** CPL-induced deracemization of overcrowded alkene-based switch **2.75** in a liquid crystalline environment. LPL = linearly polarized light, UPL = unpolarized light.

Due to the rather low helical twisting power of *M*-**2.75** ($\beta_M$ = -0.1 μm$^{-1}$ in M15) and low anisotropy factor ($g_{314}$ = -0.0064 in *n*-hexane) these effects were small and only very large cholesteric pitches could be addressed. However, it did show the potential of this system for amplification of chirality, from the handedness of circularly polarized light to a macroscopic nematic to cholesteric phase transition.

*2.4.2.4.2 Axially chiral bicyclic ketones*

In 1995, Schuster and coworkers were the first to show reversible photoswitching of a racemic bistable compound using CPL.[96] Racemic axially chiral bicyclic ketone **2.76** was irradiated with *l*-CPL, leading to partial photoresolution (Figure 2.46). Irradiation of more than 6.7 h resulted in a photostationary state with 0.4% *ee*. This value was in good agreement with the *ee* value predicted by the anisotropy factor ($g_{305}$ = 0.0105 at 305 nm), but the enantiomeric enrichment was not sufficient to cause a nematic-cholesteric phase transition, probably due to a low helical twisting power.

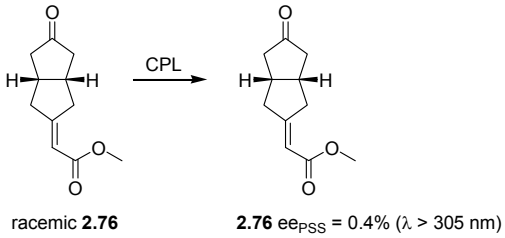


**Figure 2.46** CPL-induced deracemization of axially chiral bicyclic ketone **2.76**.

Several of these bicyclic ketones were especially designed as photochemical triggers for the control of liquid crystalline phases.[97] Due to the rigid bicyclic core and the ketone chromophore, these structures generally possess large *g*-values. Unfortunately, both the helical twisting power and solubility in nematic LC hosts are often low (Figure 2.47). Finally, the incorporation of a mesogenic unit in the switch resulted in a system capable of reversible nematic-cholesteric phase transition using circularly polarized light (Figure 2.48).[98] Switch **2.82** contains a mesogenic moiety resembling the LC host ZLI-1167 resulting in a helical twisting power of 15 μm$^{-1}$, a high *g*-value ($g_{300}$ = 0.016) and good solubility. CPL irradiation (λ > 295 nm) of a nematic mixture containing 13 mol% rac-**2.82** resulted in a cholesteric phase with a pitch of 190 μm. This was more than twice as long as the pitch obtained when a photoresolved sample at the photostationary state was doped in the mesogenic host, probably due to scattering of the CPL by the liquid crystalline mixture.

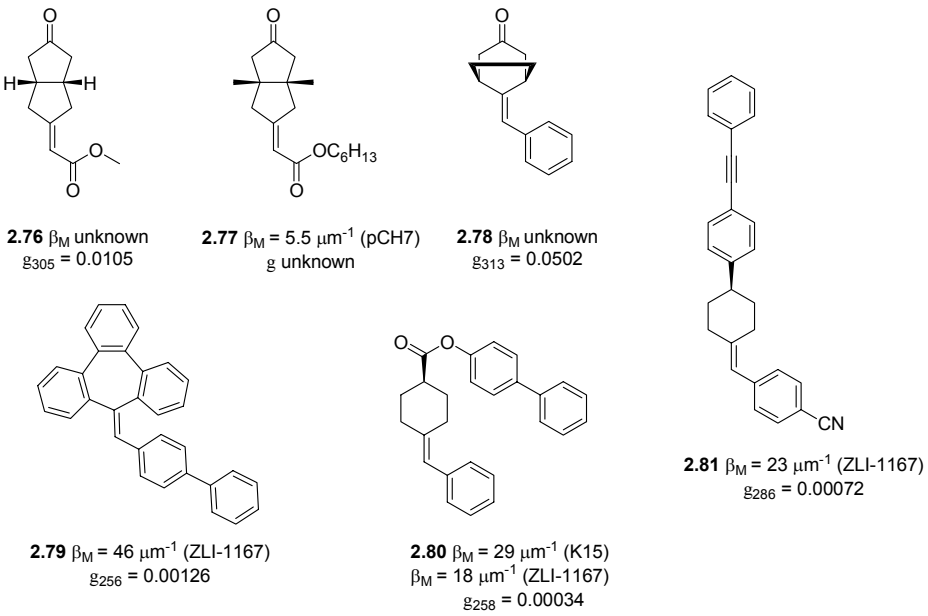


**Figure 2.47** A selection of chiral dopants developed by Schuster and coworkers.[96-98]

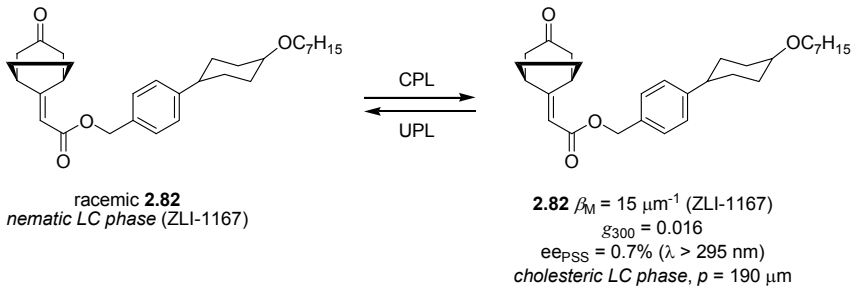


**Figure 2.48** Nematic to cholesteric phase transition by CPL irradiation of an axially chiral bicyclic ketone.

## 2.5 Conclusions

The amplification of molecular chirality by liquid crystalline systems manifests itself in chiral surface structures, helical supramolecular assemblies and several physical properties, such as optical rotation, circular dichroism and selective light

reflection. For the efficient generation of cholesteric liquid crystals several low molecular weight dopant systems with varying helical twisting powers have been developed. Among the most successful dopant classes today are TADDOLs, dioxolanes, binaphthol-based systems and chiral coordination complexes with helical twisting powers up to 400 $\mu m^{-1}$. These dopants allow the generation of sub-micrometer pitch cholesterics using millimolar quantities of chiral dopant. Although some trends in the relation between molecular structure and helical twisting power can be observed, no general rules for the design of efficient dopants have been established. The incorporation of bistable moieties in chiral dopants has led to the development of several classes of switchable chiral dopants, which allow the manipulation of sign and pitch of a cholesteric phase using an external stimulus, in particular using light. On one hand, amplification of the switch state in the chiral organization of the LC superstructure can be applied in methods for non-destructive read out. On the other hand, manipulation of the cholesteric pitch allows controlled color change of liquid crystalline films. Moreover, racemic bistable dopants can be deracemized using circularly polarized light, inducing a transition from the nematic to the cholesteric phase. The development of efficient chiral switches with high helical twisting powers of opposite sign for both switch states remains a formidable challenge that needs to be addressed if these systems are to be applied in smart materials and nano- or information technology.

## 2.6 References and Notes

[1] Or units in a polymer.

[2] F. Reinitzer, *Monatsh. Chem.* **1888**, *9*, 421.

[3] O. Lehmann, *Z. Phys. Chem.* **1889**, *4*, 462.

[4] General books on liquid crystalline research: a) I. Dierking, *Textures of Liquid Crystals*, **2003**, Wiley-VCH, Weinheim; b) *Handbook of Liquid Crystal Research*, P. J. Collins, J. S. Patel (Eds.) **1997**, Oxford University Press, New York, Oxford.; c) *Handbook of Liquid Crystals*, (Eds.: D. Demus, J. Goodby, G. W. Gray, H.-W. Spiess, V. Vill), Wiley-VCH, Weinheim, **1998**; d) *Chirality in Liquid Crystals*, H.-S. Kitzerow, C. Bahr, (Eds.), **2001**, Springer-Verlag, New York.

[5] For general information on smectic liquid crystals, see: a) J. W. Goodby in *Handbook of Liquid Crystals, Vol. 2A: Low Molecular Weight Liquid Crystals I*, Ch.5, (Eds.: D. Demus, J. Goodby, G. W. Gray, H.-W. Spiess, V. Vill), Wiley-VCH, Weinheim, **1998**; b) C. Bahr in *Chirality in Liquid Crystals*, Ch. 8, H.-S. Kitzerow, C. Bahr, (Eds.), **2001**, Springer-Verlag, New York; c) H. Takezoe, Y. Takanishi in *Chirality in Liquid Crystals*, Ch. 9, H.-S. Kitzerow, C. Bahr, (Eds.), **2001**, Springer-Verlag, New York.

[6] a) I. Dierking, *Textures of Liquid Crystals*, **2003**, Ch. 5, Wiley-VCH Weinheim; b) A. H. Hall, J. Hollingshurst, J. W. Goodby in *Handbook of Liquid Crystal Research*, Ch. 2, P. J.

Collins, J. S. Patel (Eds.) **1997**, Oxford University Press, New York, Oxford.; c) C. J. Booth in *Handbook of Liquid Crystals, Vol. 2A: Low Molecular Weight Liquid Crystals I*, Ch.4-1, (Eds.: D. Demus, J. Goodby, G. W. Gray, H.-W. Spiess, V. Vill), Wiley-VCH, Weinheim, **1998**; d) H. Coles in *Handbook of Liquid Crystals, Vol. 2A: Low Molecular Weight Liquid Crystals I*, Ch.4-2, (Eds.: D. Demus, J. Goodby, G. W. Gray, H.-W. Spiess, V. Vill), Wiley-VCH, Weinheim, **1998**; e) G. Chilaya in *Chirality in Liquid Crystals*, Ch. 6, H.-S. Kitzerow, C. Bahr, (Eds.), **2001**, Springer-Verlag, New York.

[7] J. Yoshida, H. Sato, A. Yamagishi, N. Hoshino, *J. Am. Chem. Soc.* **2005**, *127*, 8453.

[8] H. Stegemeyer, K.-J. Mainusch, *Chem. Phys. Lett.* **1970**, *6*, 5.

[9] a) M. F. Grandjean, *C. R. Acad. Sci., Paris* **1921**, 172, 71; b) R. Cano, *Bull. Soc. Fr. Mineral. Cristallogr.* **1968**, *91*, 20. c) G. Heppke, F. Oestreicher, *Mol. Cryst. Liq. Cryst.* **1977,** *41*, 245.

[10] W. Shang, M. M. Labes, *Mol. Cryst. Liq. Cryst.* **1994**, *239*, 55.

[11] Unless, of course, its wavelength is in the absorption range of a chromophore in the LC material.

[12] W. H. Bragg, W. L. Bragg, *X-Rays and Crystal Structure*, G. Bell and Sons, London, **1915**.

[13] S. Varghese, S. Narayanankutty, C. W. M. Bastiaansen, G. P. Crawford, D. J. Broer, *Adv. Mater.* **2004**, *16*, 1600.

[14] H. T. A. Wilderbeek, F. J. A. van der Meer, K. Feldman, D. J. Broer, C. W. M. Bastiaansen, *Adv. Mater.* **2002**, *14*, 655.

[15] J. Hoogboom, M. Behdani, J. A. A. W. Elemans, M. A. C. Devillers, R. de Gelder, A. E. Rowan, T. Rasing, R. J. M. Nolte, *Angew. Chem. Int. Ed.* **2003**, *42*, 1812.

[16] P. Chaudhari, J. Lacey, J. Doyle, E. Galligan, S.-C. A. Lien, A. Callegari, G. Hougham, N. D. Lang, P. S. Andry, R. John, K.-H. Yang, M. Lu, C. Cai, J. Speidell, S. Purushothaman, J. Ritsko, M. Samant, J. Stöhr, Y. Nakagawa, Y. Katoh, Y. Saitoh, K. Sakai, H. Satoh, S. Odahara, H. Nakano, J. Nakagaki, Y. Shiota, *Nature* **2001**, *411*, 56.

[17] a) W. M. Gibbons, P. J. Shannon, S.-T. Sun, B. J. Swetlin, *Nature* **1991**, *351*, 49; b) M. Schadt, H. Seiberle, A. Schuster, *Nature* **1996**, *381*, 212;

[18] I. Dierking, *Textures of Liquid Crystals*, **2003**, Ch. 3, Wiley-VCH, Weinheim.

[19] For reviews on chiral low molecular weight dopants: a) G. Solladié, R. G. Zimmermann, *Angew. Chem. Int. Ed. Engl.* **1984**, *23*, 348; b) G. P. Spada, G. Proni, *Enantiomer* **1998**, *3*, 301; c) G. Proni, G. P. Spada, *Enantiomer* **2001**, *6*, 171.

[20] For reviews on switching in liquid crystalline environments, see: a) K. Ichimura, *Chem. Rev.* **2000**, *100*, 1847; b) T. Ikeda, A. Kanazawa in *Molecular Switches*, B.L. Feringa (Ed.), **2001**, Wiley-VCH, p 363-397; c) N. Tamaoki, *Adv. Mater.* **2001**, *13*, 1135; d) T. Ikeda, *J. Mater. Chem.* **2003**, *13*, 2037.

[21] In this thesis, mesogenic groups are defined as functional groups that resemble the main structure of the mesogenic host, which is in accordance with IUPAC nomenclature. See *Pure Appl. Chem.* **2001**, *73*, 845.

[22] H. Finkelmann, H. Stegemeyer, *Ber. Bunsenges. Phys. Chem.* **1978**, *82*, 1302.

[23] G. P. Semenkova, L. A. Kutulya, N. I. Shkol'nikova, T. V. Khandrimailova, *Cryst. Rep.* **2001**, *46*, 118.

[24] a) H.-G. Kuball, H. Brüning, T. Müller, O. Türk, A. Schönhofer, *J. Mater. Chem.* **1995**, *5*, 2167; b) H.-G. Kuball, H. Brüning, *Chirality* **1997**, *9*, 407.
[25] R. A. van Delden, B. L. Feringa, *Angew. Chem. Int. Ed.* **2001**, *40*, 3198.
[26] P. L. Rinaldi, M. S. R. Naidu, W. E. Conaway, *J. Org. Chem.* **1982**, *47*, 3987.
[27] P. L. Rinaldi, M. Wilk, *J. Org. Chem.* **1983**, *48*, 2141.
[28] R. A. van Delden, B. L. Feringa, *Chem. Commun.* **2002**, 174.
[29] R. Eelkema, R. A. van Delden, B. L. Feringa, *Angew. Chem. Int. Ed.* **2004**, *43*, 5013.
[30] N. Hoshino, Y. Matsuoka, K. Okamoto, A. Yamagishi, *J. Am. Chem. Soc.* **2003**, *125*, 1718.
[31] N. Anzai, S. Machida, K. Horie, *Liq. Cryst.* **2003**, *30*, 359.
[32] G. Gottarelli, G. P. Spada, *Mol. Cryst. Liq. Cryst.* **1985**, *123*, 377.
[33] S. Zahn, G. Proni, G. P. Spada, J. W. Canary, *Chem. Eur. J.* **2001**, *7*, 88.
[34] TADDOL = α,α,α',α'-tetraaryl-2,2-dimethyl-1,3-dioxolan-4,5-dimethanol; for a review see D. Seebach, A. K. Beck, A. Heckel, *Angew. Chem. Int. Ed.* **2001**, *40*, 92.
[35] Nematic LC host ZLI-1695 is a eutectic mixture with a structure similar to ZLI-1167 (see Table 2.1) and n = 1, 2, 3, 6; Phase transition temperatures were not available.
[36] H.-G. Kuball, B. Weiss, A. K. Beck, D. Seebach, *Helv. Chim. Acta* **1997**, *80*, 2507.
[37] A. J. Seed, M. E. Walsh, J. W. Doane, A. Khan, *Mol. Cryst. Liq. Cryst.* **2004**, *410*, 201.
[38] a) C. Rosini, G. P. Spada, G. Proni, S. Masiero, S. Scamuzzi, *J. Am. Chem. Soc.* **1997**, *119*, 506; b) S. Superchi, M. I. Donnoli, G. Proni, G. P. Spada, C. Rosini, *J. Org. Chem.* **1999**, *64*, 4762.
[39] G. Gottarelli, G. P. Spada, R. Bartsch, G. Solladié, R. G. Zimmermann, *J. Org. Chem.* **1986**, *51*, 589.
[40] G. Solladié, G. Gottarelli, *Tetrahedron* **1987**, *43*, 1425.
[41] A. Ferrarini, G. J. Moro, P. L. Nordio, *Phys. Rev. E* **1996**, *53*, 681.
[42] The authors use *M* and *P* helicities when describing these systems, which is in conflict with IUPAC nomenclature. Therefore, these relative helicities will be designated pseudo-*M* (*M'*) and pseudo-*P* (*P'*) in this thesis.
[43] G. Gottarelli, M. Hibert, B. Samori, G. Solladié, G. P. Spada, R. Zimmermann, *J. Am. Chem. Soc.* **1983**, *105*, 7318.
[44] C. Rosini, I. Rosati, G. P. Spada, *Chirality* **1995**, *7*, 353.
[45] H. J. Deussen, P. V. Shibaev, R. Vinokur, T. Bjornholm, K. Schaumburg, K. Bechgaard, V. P. Shibaev, *Liq. Cryst.* **1996**, *21*, 327.
[46] M. Bandini, S. Casolari, P. G. Cozzi, G. Proni, E. Schmohel, G. P. Spada, E. Tagliavini, A. Umani Ronchi, *Eur. J. Org. Chem.* **2000**, 491.
[47] G. Proni, G. P. Spada, P. Lustenberger, R. Welti, F. Diederich, *J. Org. Chem.* **2000**, *65*, 5522.
[48] G. Gottarelli, G. Proni, G. P. Spada, D. Fabbri, S. Gladiali, C. Rosini, *J. Org. Chem.* **1996**, *61*, 2013.
[49] G. Gottarelli, G. P. Spada, G. Solladié, *Nouv. J. Chim.* **1986**, *10*, 691.
[50] V. E. Williams, R. P. Lemieux, *Chem. Commun.* **1996**, 2259.
[51] A. di Matteo, S. M. Todd, G. Gottarelli, G. Solladié, V. E. Williams, R. P. Lemieux, A. Ferrarini, G. P. Spada, *J. Am. Chem. Soc.* **2001**, *123*, 7842.

[52] G. Gottarelli, H.-J. Hansen, G. P. Spada, R. H. Weber, *Helv. Chim. Acta* **1987**, *70*, 430.
[53] W. Bernhard, P. Brügger, J. J. Daly, G. Englert, P. Schönholzer, H.-J. Hansen, *Helv. Chim. Acta* **1985**, *68*, 415.
[54] a) R. Holzwarth, R. Bartsch, Z. Cherkaoui, G. Solladié, *Chem. Eur. J.* **2004**, *10*, 3931; b) R. Holzwarth, R. Bartsch, Z. Cherkaoui, G. Solladié, *Eur. J. Org. Chem.* **2005**, 3536.
[55] The molecular structure of LC host ROTN 3010 is unavailable.
[56] G. Heppke, D. Lötzsch, F. Oestreicher, *Z. Naturforsch.* **1986**, *41a*, 1214. The $\beta$-value was reported in $m^2$/mol for LC host ROTN 404, a mixture of biphenylpyrimidines of unknown composition, which makes exact recalculation to $\beta_M$ troublesome.
[57] K. Akagi, G. Piao, S. Kaneko, K. Sakamaki, H. Shirakawa, M. Kyotani, *Science* **1998**, *282*, 1683.
[58] T. Mori, T. Sato, M. Kyotani, K. Akagi, *Synth. Metals* **2003**, *135-136*, 83.
[59] K. Kanazawa, I. Higuchi, K. Akagi, *Mol Cryst. Liq. Cryst.* **2001**, *364*, 825.
[60] J. Cheung, L. D. Field, S. Sternhell, *J. Org. Chem.* **1997**, *62*, 7044.
[61] Special issue of *Scientific American: Nanotech, The Science of the Small Gets Down to Business*, September **2001**.
[62] For reviews, see: a) V. Balzani, A. Credi, F. M. Raymo, J. F. Stoddart, *Angew. Chem. Int. Ed.* **2000**, *39*, 3348; b) B. L. Feringa (ed.), *Molecular Switches*, Wiley-VCH, **2001**, Weinheim; c) The May **2000** issue of *Chem. Rev.*: Memories and Switches.
[63] F. L. Carter, H. Siatkowski, H. Wohltgen, *Molecular Electronic Devices*, Elsevier, Amsterdam, **1988**.
[64] Selected examples: a) M. Moriyama, S. Song, H. Matsuda, N. Tamaoki, *J. Mater. Chem.* **2001**, *11*, 1003; b) S. Kurihara, T. Kanda, T, Nagase, T. Nonaka, *Appl. Phys. Lett.* **1998**, *73*, 2081; c) N. Tamaoki, S. Song, M. Moriyama, H. Matsuda, *Adv. Mater.* **2000**, *12*, 94; d) S. V. Serak, E. O. Arikainen, H. F. Gleeson, V. A. Grozhik, J.-P. Guillou, N. A. Usova, *Liq. Cryst.* **2002**, *29*, 19.
[65] S. Tazuke, S. Kurihara, T. Ikeda, *Chem. Lett.* **1987**, 911.
[66] E. Sackmann, *J. Am. Chem. Soc.* **1971**, *93*, 7088.
[67] a) C. Ruslim, M. Nakagawa, S. Morino, K. Ichimura, *Mol. Cryst. Liq. Cryst.* **2001**, *365*, 55; b) T. Yoshioka, M. D. Z. Alam, T. Ogata, T. Nonaka, S. Kurihara, *Liq. Cryst.* **2004**, *31*, 1285; c) S. Kurihara, S. Nomiyama, T. Nonaka, *Chem. Mater.* **2000**, *12*, 9; d) S. Kurihara, S. Nomiyama, T. Nonaka, *Chem. Mater.* **2001**, *13*, 1992; e) C. Ruslim, K. Ichimura, *J. Phys. Chem. B.* **2000**, *104*, 6529.
[68] R. A. van Delden, T. Mecca, C. Rosini, B. L. Feringa, *Chem. Eur. J.* **2004**, *10*, 61.
[69] a) S. Pieraccini, S. Masiero, G. P. Spada, G. Gottarelli, *Chem. Commun.* **2003**, 598 ; b) S. Pieraccini, G. Gottarelli, R. Labruto, S. Masiero, O. Pandoli, G. P. Spada, *Chem. Eur. J.* **2004**, *10*, 5632.
[70] Nematic LC host Phase 1052 is a mixture with a structure similar to ZLI-389 (see Table 2.1). The exact composition and phase transition temperatures were not available.
[71] a) C. Ruslim, K. Ichimura, *Adv. Mater.* **2001**, *13*, 37; b) C. Ruslim, K. Ichimura, *J. Mater. Chem.* **2002**, *12*, 3377.

[72] E44 is a nematic mixture of cyanobiphenyls, similar to E7; DON-103 is a nematic mixture of cyclohexanecarboxylic acid phenyl esters.
[73] a) H.-K. Lee, K. Doi, H. Harada, O. Tsutsumi, A. Kanazawa, T. Shiono, T. Ikeda *J. Phys. Chem. B* **2000**, *104*, 7023; b) A. Y. Bobrovsky, N. I. Boiko, V. P. Shibaev, J. Springer, *Adv. Mater.* **2000**, *12*, 1180.
[74] Nematic LC host ZLI-2359 is a mixture with a structure similar to ZLI-1167 (see Table 2.1). The exact composition and phase transition temperatures are not available.
[75] Due to overlap in the absorption spectra of the *E* and *Z* isomers, no complete conversion of one isomer to the other can be achieved by irradiation. As a result of this, the helical twisting powers of the photostationary states (PSS) are reported. Moreover, the presence of two azobenzene moieties makes the PSS composition even more complex.
[76] E48 is a nematic mixture of cyanobiphenyls, similar to E7. The exact composition and phase transition temperatures are not available.
[77] P. M. A. Bonaccorsi, D. A. Dunmur, J. F. Stoddart, *New. J. Chem.* **1988**, *12*, 83.
[78] S. N. Yarmolenko, L. A. Kutulya, V. V. Vashchenko, L. V. Chepeleva, *Liq. Cryst.* **1994**, *16*, 877.
[79] M. Brehmer, J. Lub, P. van de Witte, *Adv. Mater.* **1998**, *10*, 1438.
[80] M. Irie, *Chem. Rev.* **2000**, *100*, 1685.
[81] C. Denekamp, B. L. Feringa, *Adv. Mater.* **1998**, *10*, 1080.
[82] a) T. Yamaguchi, T. Inagawa, H. Nakazumi, S. Irie, M. Irie, *Chem. Mater.* **2000**, *12*, 869; b) T. Yamaguchi, T. Inagawa, H. Nakazumi, S. Irie, M. Irie, *Mol. Cryst. Liq. Cryst.* **2001**, *365*, 861; c) T. Yamaguchi, T. Inagawa, H. Nakazumi, S. Irie, M. Irie, *Mol. Cryst. Liq. Cryst.* **2000**, *345*, 287; d) T. Yamaguchi, T. Inagawa, H. Nakazumi, S. Irie, M. Irie, *J. Mater. Chem.* **2001**, *11*, 2453.
[83] Y. Yokoyama, *Chem. Rev.* **2000**, *100*, 1717.
[84] a) Y. Yokoyama, T. Sagisaka, *Chem. Lett.* **1997**, 687; b) T. Sagisaka, Y. Yokoyama, *Bull. Chem. Soc. Jpn.* **2000**, *73*, 191.
[85] For stereochemical definitions, see: E. L. Eliel, S. H. Wilen, *Stereochemistry of Organic Compounds*, Wiley, New York, **1994**.
[86] B. L. Feringa, N. P. M. Huck, H. A. van Doren, *J. Am. Chem. Soc.* **1995**, *117*, 9929.
[87] N. P. M. Huck, *Ph.D. Thesis*, University of Groningen, **1997**.
[88] Nematic LC host M15 is 4'-pentyloxybiphenylnitrile, with C-N and N-I transition temperatures of 48 and 67 °C, respectively.
[89] R. A. van Delden, M. B. van Gelder, N. P. M. Huck, B. L. Feringa, *Adv. Funct. Mater.* **2003**, *13*, 319.
[90] R. A. van Delden, *Ph.D. Thesis*, University of Groningen, **2002**.
[91] C.-T. Chen, Y.-C. Chou, *J. Am. Chem. Soc.* **2000**, *122*, 7662.
[92] N. Koumura, R. W. J. Zijlstra, R. A. van Delden, N. Harada, B. L. Feringa, *Nature* **1999**, *401*, 152.
[93] R. A. van Delden, N. Koumura, N. Harada, B. L. Feringa, *Proc. Nat. Acad. Sci. USA* **2002**, *99*, 4945.

[94] Exceptions to the rule can be found among certain photoactive chiral chromium complexes, see for instance K. L. Stevenson, J. F. Verdieck, *J. Am. Chem. Soc.* **1968**, *90*, 2974.
[95] N. P. M. Huck, W. F. Jager, B. de Lange, B. L. Feringa, *Science* **1996**, *273*, 1686.
[96] M. Suarez, G. B. Schuster, *J. Am. Chem. Soc.* **1995**, *117*, 6732.
[97] a) Y. Zhang, G. B. Schuster, *J. Am. Chem. Soc.* **1994**, *116*, 4852; b) Y. Zhang, G. B. Schuster, *J. Org. Chem.* **1995**, *60*, 7192; c) R. Lemieux, G. B. Schuster, *J. Org. Chem.* **1993**, *58*, 100; d) B. S. Udayakumar, G. B. Schuster, *J. Org. Chem.* **1993**, *58*, 4165; e) Y. Zhang, G. B. Schuster, *J. Org. Chem.* **1994**, *59*, 1855.
[98] K. S. Burnham, G. B. Schuster, *J. Am. Chem. Soc.* **1999**, *121*, 10245.